Progress in Oceanography 206 (2022) 102809

Contents lists available at ScienceDirect

Progress in Oceanography

journal homepage: www.elsevier.com/locate/pocean

Planktonic protist diversity across contrasting Subtropical and Subantarctic waters of the southwest Pacific

Andres Gutiérrez-Rodríguez [a,*], Adriana Lopes dos Santos [b], Karl Safi [c], Ian Probert [d], Fabrice Not [e], Denise Fernández [a], Priscillia Gourvil [d], Jaret Bilewitch [a], Debbie Hulston [a], Matt Pinkerton [a], Scott D. Nodder [a]

[a] National Institute of Water and Atmospheric Research, Wellington, New Zealand
[b] Asian School of the Environment, Nanyang Technological University, 50 Nanyang Avenue, Singapore, 639798, Singapore
[c] National Institute of Water and Atmospheric Research, Hamilton, New Zealand
[d] Sorbonne Universités, Sorbonne Université, CNRS, FR2424 Station Biologique de Roscoff, France
[e] Sorbonne University, CNRS, UMR7144, Ecology of Marine Plankton Team, Station Biologique de Roscoff, France

ARTICLE INFO

Keywords:
Planktonic protist
Taxonomic diversity
18S rRNA metabarcoding
Biogeography
Southwest Pacific
Subtropical
Subantarctic
Subtropical Front

ABSTRACT

Planktonic protists are an essential component of marine pelagic ecosystems where they mediate important trophic and biogeochemical functions. Although these functions are largely influenced by their taxonomic affiliation, the composition and spatial variability of planktonic protist communities remain poorly characterized in vast areas of the ocean. Here, we investigated the diversity of these communities in contrasting oceanographic conditions of the southwest Pacific (33–58 °S) using DNA metabarcoding of the 18S rRNA gene. Seawater samples collected during twelve cruises (n = 482, 0–3100 m) conducted east of New Zealand were used to characterize protist communities in Subtropical (STW) and Subantarctic (SAW) surface water masses and the Subtropical Front (STF) that separates them. Diversity decreased with increasing latitude and increasing temperature but tended to be lowest in the STF. Sample ordination resulting from the abundance of amplicon single variants (ASVs) corresponded to the different water masses. Overall, *Dinoflagellata* (Syndiniales, 27%; *Dinophyceae*, 24% of standardized number of reads) dominated the euphotic zone followed by Chlorophyta (20%), but their relative abundance and composition at class and lower taxonomic levels varied consistently between water masses. Among Chlorophyta, several picoplanktonic algae species of the *Mamiellophyceae* class including *Ostreococcus lucimarinus* dominated in STW, while the *Chloropicophyceae* species *Chloroparvula pacifica* was most abundant in SAW. *Bacillariophyta* (5%), *Prymnesiophyceae* (5%), and *Pelagophyceae* (2%) classes were less abundant but showed analogous water mass specificity at class and finer taxonomic levels. Protist community composition in the STF had mixed characteristics and showed regional differences with the southern STF (50 °S) having more resemblance with subantarctic communities than the STF over the Chatham Rise region (42–44 °S). Below the euphotic zone, Syndiniales sequences (40%) dominated the dataset followed by Radiolaria (31%), *Dinophyceae* (14%) and other heterotrophic groups like Marine Stramenopiles and ciliates (1–1.5%). Among Radiolaria, several unidentified ASVs assigned to *Spumellaria* were most abundant, but showed significantly different distributions between STW and SAW highlighting the need to further investigate the taxonomy and ecology of this group. The present study represents a significant step forward towards characterizing protistan communities composition in relation to major physical oceanographic features in the southwest Pacific providing new insights about the biogeography and ecological preferences of different planktonic protist taxa from class to species and genotypic level.

1. Introduction

Planktonic protists, including phototrophic, heterotrophic and mixotrophic single-celled eukaryotes, have key roles in the functioning of marine ecosystems (Caron et al., 2012). Phytoplankton are responsible for 50% of global primary productivity (Field et al., 1998). Most of this primary production is consumed and processed by heterotrophic protists (i.e. microzooplankton) before becoming available for larger

* Corresponding author.
E-mail address: andres.gutierrez@ieo.csic.es (A. Gutiérrez-Rodríguez).

https://doi.org/10.1016/j.pocean.2022.102809
Received 12 September 2021; Received in revised form 8 April 2022; Accepted 25 April 2022
Available online 25 May 2022

zooplankton and higher trophic levels (Calbet and Landry, 2004; Calbet and Saiz, 2005; Zeldis and Décima, 2020). From a biogeochemical perspective, the microbial production, consumption and remineralization of organic matter is at the core of global biogeochemical cycles including the nitrogen and carbon cycles, and is pivotal in regulating the ocean's capacity to sequester atmospheric CO_2 via the biological carbon pump (Turner, 2015; Boyd et al., 2019).

The trophic and biogeochemical processes driven by microbial communities are influenced by their taxonomic composition, which is tightly coupled to physico-chemical conditions. With increasing evidence of climate change effects on the physico-chemical status of the ocean (e.g. warming, increased stratification and reduced nutrient supply, deoxygenation, acidification) (Sarmiento et al., 2004; Pörtner et al., 2014; Henley et al., 2020) it becomes imperative to better characterize the biogeography and distributions of microbial communities in relation to oceanographic provinces (Cavicchioli et al., 2019). This is required to establish a conceptual framework and baselines upon which future environmental change can be evaluated.

The diversity and dynamic nature of microbial communities has precluded a comprehensive characterization of species composition and distributional patterns across relevant temporal and spatial scales (Wietz et al., 2019). Extensive application of DNA metabarcoding approaches during the last 10 years have contributed significantly to this end by characterizing the diversity of marine protist communities over a wide range of temporal and spatial scales with unprecedented taxonomic resolution and coverage (Santoferrara et al., 2020). Only a few studies have applied DNA metabarcoding approaches to investigate protist community and species diversity changes across oceanic fronts in the southwest (SW) Pacific (Raes et al., 2018; Allen et al., 2020; Sow et al., 2020). Despite these efforts vast ocean regions in the SW Pacific Ocean, remain largely unexplored with regards to the characterization of protist community composition and spatial distribution of major taxonomic groups. This study contributes to fill this gap by using high-throughput DNA sequencing to investigate protist communities in relation to major water masses and oceanographic fronts characteristic of the SW Pacific waters east of Aotearoa New Zealand (Fig. 1).

Spanning latitudes of 55 °S and 35 °S, New Zealand's continental mass interrupts the converging flows of the South Pacific subtropical gyre and the northward excursions of the Antarctic Circumpolar Current (ACC). The mixing of the warm and saltier subtropical surface water (STW) with the cold, relatively fresh subantarctic surface water (SAW) (Boyd et al., 1999) results in the genesis of oceanic fronts and semi-permanent eddies with distinctive signatures in water properties extending along the eastern margin off Aotearoa New Zealand (Chiswell et al., 2015; Fernandez et al., 2018). To the north, the East Auckland Current (EAUC) brings STW sourced partially from the western limb of the South Pacific subtropical gyre as the Tasman Front (Sutton and Bowen, 2014) and interacts with a series of semi-permanent eddies along the eastern margin of Aotearoa New Zealand (Roemmich and Sutton, 1998; Santana et al., 2021). At about 37 °S, on the eastern side of Te Ika a Māui North Island the EAUC turns south to become the East Cape Current (Stanton et al., 1997) extending the STW inflow to the Chatham Rise where it separates from the coast to the east, forming the semi-permanent Wairarapa Eddie (Roemmich and Sutton, 1998; Chiswell, 2013) and the northern edge of the Subtropical Front (STF) (Deacon, 1982; Heath, 1985; Chiswell et al., 2015). The STF is characterized by strong temperature gradients and a sharp salinity contrast that intensifies near the rise (Sutton, 2001; Chiswell, 2001), up to 4 °C and 0.7 practical salinity units, respectively, over 1° latitude in this region (Belkin and Gordon, 1996). This transitional zone separating waters of subtropical origin from the subantarctic is known as the Subtropical Frontal Zone (SFTZ) (Deacon, 1982) and it is bounded by the northern (N-STF) and southern (S-STF) branches of the STF. The STFZ can be up to 500 km wide in the Tasman Sea region before it gets constricted around the South Island of New Zealand where gradients set in motion, guided by the continental slope (Smith et al., 2013), the geostrophic flow associated with the S-STF branch and its coastal expression, the Southland Current (SC) along the western continental slope of Te Waipounamu South Island. The mean transport of the SC is about 8 Sv (1 Sv = 10^6 m^3s^{-1}) with 10% corresponding to STW and 90% to SAW (Sutton, 2003). The SC advects this mix of neritic STW and SAW northwards off the east coast and reaches south of the Chatham Rise at the Mernoo Gap and the northern edge of the Bounty Trough. Further east and along the flanks of Campbell Plateau, the flows associated with the Subantarctic Front (SAF) carry the largest portion of SAW, about 50 Sv into the region southeast of the Chatham Rise (Stanton and Morris, 2004; Bowen et al., 2014). Access of SAW onto the plateau from the east occurs through the bathymetric gaps, saddles and ridges where waters then become isolated from the neighbouring circulation and contribute significantly to the development of oceanographic and climatic processes such as subantarctic mode water formation (Forcén-Vázquez et al., 2021). Southeast of the Chatham Rise and away from the plateau in the SW Pacific the STFZ re-emerges as a 150 km wide band with the typical signatures of the STF-N and STF-S fronts (Sutton, 2001; Behrens et al., 2021).

STW and SAW have contrasting biogeochemical characteristics (Heath, 1985; Bradford-Grieve et al., 1999; Chiswell et al., 2015; Boyd et al., 1999; Sherlock et al., 2007). North of Aotearoa New Zealand, STW is oligotrophic (low macro- and micronutrients) and phytoplankton production is considered to be limited by nitrogen (Zentara and Kamykowski, 1981) with pervasive nitrogen-fixation by diazotrophs (Law et al., 2012; Ellwood et al., 2018). The STF is a dynamic region, characterized by strong temperature and salinity gradients (Sutton, 2001) where high levels of vertical and lateral mixing of nitrogen-limited STW and macronutrient-rich SAW (Chiswell, 2001), leads to regionally elevated annual net primary production (Murphy et al., 2001; Pinkerton et al., 2005). In SAW iron is the primary limiting nutrient for phytoplankton growth (Banse, 1996; Boyd et al., 1999) although silicate and light can become limiting at times in SAW extending southeast of Aotearoa New Zealand resulting in this being regarded as high-nutrient, low-chlorophyll, low-silicate (HNLC-LSi) region (Dugdale et al., 1996; Boyd et al., 2010). These conditions are typically associated with SAW north of the Subantarctic Front (SAF), which is an oceanic area commonly referred to as the Subantarctic Zone (SAZ) (Trull et al., 2001) or the Subantarctic Water Ring (Longhurst, 2007). In the SAZ, increasing availability of dissolved silica southwards shifts the Polar Frontal Zone extending between the SAF and the Polar Front to 'standard' Southern Ocean HNLC conditions (Rigual-Hernández et al., 2015).

Several studies have characterized microbial community composition in STW and SAW east of New Zealand, using microscopy (Chang and Gall, 1998), pigments (Delizo et al., 2007) and flow-cytometry (Hall et al., 2001). These regional studies have focused mainly on the STFZ or coastal communities (Chang et al., 2003; Hall et al., 2006), while studies analysing wider phytoplankton distributions across STW and SAW have targeted specific groups such as coccolithophores (Saavedra-Pellitero et al., 2014; Chang and Northcote, 2016). More process-oriented studies have also provided partial information on phytoplankton composition in SAW and STW east of New Zealand (Peloquin et al., 2011; Ellwood et al., 2013; Chiswell et al., 2019). These studies have described the prevalence of larger cells and diatoms through winter and spring in the more productive waters of the STF, compared to STW and SAW (Chang and Gall, 1998; Bradford-Grieve et al., 1999). Diatom- and autotrophic flagellate-dominated communities have been reported in STW on the northern flank of the Chatham Rise during spring while dinoflagellates and small flagellates are documented as dominating the eukaryotic phytoplankton in SAW (Bradford-Grieve et al., 1997; Chang and Gall, 1998). Diatom and coccolithophore species composition of sediment trap fluxes on the northern (STW-influenced) and southern (SAW-influenced) flanks of the Chatham Rise highlight the importance of these phytoplankton groups in the region (Wilks et al., 2021). However, there is surprisingly

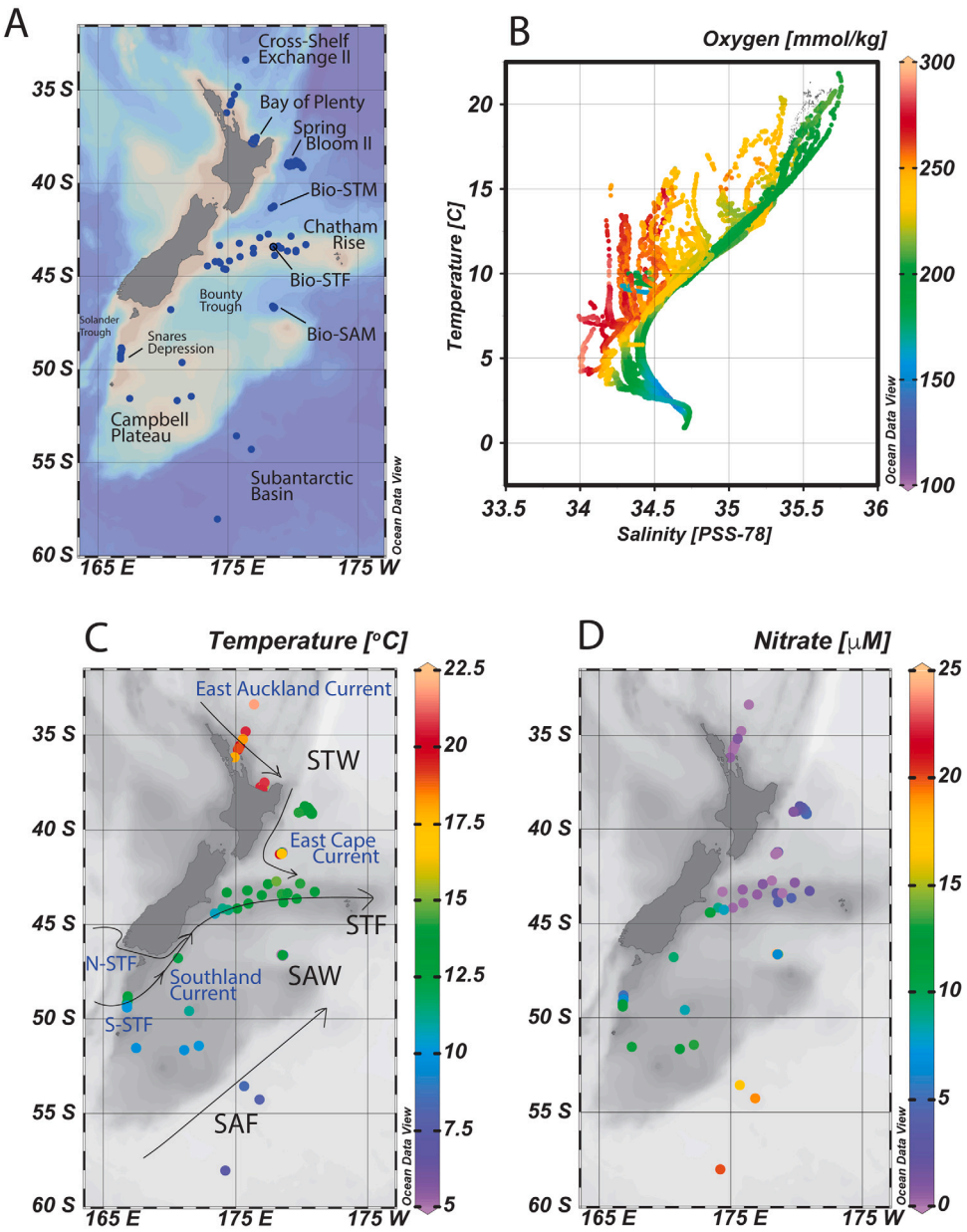

Fig. 1. Study area. (A) Map of the study area with the sampling sites locations. (B) T–S diagram with oxygen concentration. Surface (10 m) (C) temperature and (D) nitrate concentration at sampling sites in relation to major water masses and currents and fronts of the study region (Chiswell et al., 2015). Bio-SAM, Bio-STF, and Bio-STM refers to Biophysical Moorings program sampling sites in Subantarctic (SAW), Subtropical (STW) and Subtropical Front (STF) and Subantarctic Front (SAF) waters. North (STF) and South Subtropical Front (S-STF) designations adapted from Smith et al. (2013) around southern New Zealand and on the Chatham Rise (Sutton, 2001), east of Aotearoa New Zealand.

only little information available on the taxonomic composition of phytoplankton communities prevailing in open-ocean waters away from the STFZ over the Chatham Rise region (Peloquin et al., 2011; Twining et al., 2014; Chang and Northcote, 2016; Chiswell et al., 2019). Further east of this region (170 °W), phytoplankton community composition from polar to equatorial waters have been characterized using pigment analysis (DiTullio et al., 2003) whereas a more recent study applied DNA metabarcoding analysis to investigate microbial diversity patterns in relation to physico-chemical gradients and oceanographic features (Raes et al., 2018). DNA metabarcoding has also been recently applied to investigate protist diversity changes across the Southland Current (Allen et al., 2020). However, the full taxonomic composition of protistan communities associated with open-ocean surface water masses in the SW Pacific and across major oceanographic fronts that separate them is still lacking.

The aims of the present study are: (1) to characterize the diversity of protistan communities in STW and SAW east of New Zealand and across the STFZ that separates these water masses, and (2) to investigate the spatial distributional patterns of the main protistan taxonomic groups and species in relation to physical and chemical variability of the main water masses east of Aotearoa New Zealand. Specifically, we want to know how (dis-)similar are protist communities in the biogeochemically contrasting STW and SAW? What are the main environmental factors responsible for these differences? Which are the main taxonomic groups associated with each water mass and their environmental preferences? To do so we have applied DNA metabarcoding analysis (18S rRNA) to >450 samples collected during 12 oceanographic voyages conducted over several years (2009–2017) and different seasons across STW and SAW east of New Zealand. This sequence data together with core physico-chemical and biological parameters (e.g. temperature, salinity, mixed-layer depth (MLD), macronutrients, total and

Table 1
Summary of cruises from which samples were collected. Information includes cruise identification code, start and end dates of sampling, project name, water masses covered, latitudinal range, season, region or site, number of stations and samples collected in each cruise and range of sampling depth in meters.

Cruise	Start	End	Project	Water mass	min Lat	max Lat	Season	Region or Site	N stations	N Samples	Depth range
TAN0902	30-01-09	03-02-09	BiophysMoorings	SAW // STF // STW	−46.62	−41.23	Summer	Bio-SAM // Bio-STF //Bio-STM	3	28	10-1500
TAN0909	27-10-09	30-10-09	BiophysMoorings	SAW // STF // STW	−46.64	−41.2	Spring	Bio-SAM // Bio-STF //Bio-STM	3	32	10-2764
TAN1006	06-05-10	08-05-10	BiophysMoorings	SAW // STF // STW	−46.64	−41.19	Autumn	Bio-SAM // Bio-STF //Bio-STM	3	33	10-3100
TAN1103	19-02-11	21-02-11	BiophysMoorings	SAW // STF // STW	−46.61	−41.31	Summer	Bio-SAM // Bio-STF //Bio-STM	3	34	10-3074
TAN1113	29-09-11	01-10-11	BiophysMoorings	SAW // STF // STW	−46.63	−41.22	Spring	Bio-SAM // Bio-STF //Bio-STM	3	34	10-3092
TAN1203	17-02-12	05-03-12	SOAP	STF	−44.61	−43.48	Summer	Chatham Rise	10	10	2
TAN1204	19-03-12	21-03-12	BiophysMoorings	SAW // STF // STW	−46.64	−41.26	Autumn	Bio-SAM // Bio-STF //Bio-STM	4	32	10-3100
TAN1212	19-09-12	05-10-12	Spring Bloom II	STW	−37.87	−37.51	Spring	Spring Bloom	19	105	100-300
KAH1303	08-03-13	14-03-13	Bay of Plenty	STW	−39.17	−38.76	Autumn	Bay of Plenty	12	37	2-192
TAN1516	05-12-15	21-12-15	Fisheries Oceanography IV	STF	−44.42	−42.72	Summer	Chatham Rise	20	39	7
TAN1604	14-05-16	21-05-17	Cross-shelf Exchange	STW	−36.18	−33.38	Autumn	Cross-shelf Exchange	7	42	10-110
TAN1702	18-03-17	29-03-17	Campbell Plateau	SAW	−54.26	−46.77	Autumn	Campbell Plateau	13	52	5-100
TAN1802	13-02-18	13-02-18	SO-RossSea	SAW	−58.03	−58.03	Summer	Subantarctic Basin	1	5	25-200

size-fractionated chlorophyll *a* provides the most comprehensive dataset of protistan plankton diversity in STW and SAW in the SW Pacific and contributes significantly towards building a robust baseline against which future changes in the region can be evaluated.

2. Methods

2.1. Study area and sample collection

Seawater samples and data were collected during 12 research cruises conducted in SW Pacific waters east of Aotearoa New Zealand between 2009 and 2017 (Fig. 1). Six of these cruises were conducted as part of the Biophysical Moorings long-term monitoring project (BiophysMoorings) (Nodder et al., 2016) that revisited the same sites in STW (Bio-STM), STF (Bio-STF) and SAW (Bio-SAM) (Nodder et al., 2016) through time. The rest of the cruises providing data to the present study represent single cruises to the specific region, typically focusing on a process of interest (Table 1). The dataset covers 100 stations distributed between 54.3 and 33.4 °S with seawater samples (n = 482) collected over the 0–3100 m depth range and covering spring, summer and autumn periods (Table 1). The number of DNA samples from STW (n = 271) were 2-fold higher than those from SAW (n = 121) and STF (n = 91) mainly due to the large number of samples from the Spring Bloom II cruise (TAN1212, Chiswell et al., 2019) (Table 1). Details about latitudinal and seasonal coverage of each water mass and the sample density distribution of analysed DNA samples, together with physico-chemical variables, are shown in Figure S2. The seasonality coverage was similar among the three different regions (STW, SAW, STF) but was biased against winter with most samples collected during spring, summer and autumn periods. (Table 1; Figure S1). While the sampling strategy of the present study precluded a robust seasonal analysis – with different regions sampled at different times – some aspects of temporal variability were investigated from the six Biophysical Mooring cruises that visited the same sites (Bio-SAM, Bio-STF, and Bio-STM) twice every season except winter (Table 1).

Samples were collected from 10 L Niskin bottles attached to a water bottle rosette in association with a Seabird 9plus CTD, equipped with temperature, salinity, dissolved oxygen, fluorometer, beam transmissometer and a photosynthetically active radiation (PAR) sensors (Biospherical Instruments QCP-2300L-HP). Because many CTD casts were conducted predawn K_dPAR was estimated from chlorophyll *a* (Chl *a*) (Morel and Maritorena, 2001). The euphotic zone depth (Zeu) was defined as the depth where downwelling PAR irradiance was 1% of incident irradiance (E_0). The mixed-layer depth (MLD) was defined as the shallowest depth where density exceeded the 5 m value by 0.03 kg/m^3 (Gardner et al., 1995). During the TAN1516 voyage in the STFZ of the Chatham Rise, samples were collected with a Niskin bottle deployed manually down to 10 m depth and from the R/V *Tangaroa* Underway Flow-Through System (TUFTS) system equipped with temperature, salinity, and fluorescence sensors. Seawater samples for nutrients, Chl *a* and DNA were sampled from the Niskin bottles using acid-washed silicone tubing and filtered through different types of filters for processing, as outlined below.

2.2. Nutrients, total and size-fractionated chlorophyll a

Samples for nutrients were filtered through 25 mm-diameter Whatman GF/F filters into clean 250 ml polyethylene bottles and frozen at −20 °C until analysis using an Astoria Pacific API 300 microsegmented flow analyser (Astoria-Pacific, Clackamas, OR, United States) according to the colorimetric methods described in Law et al. (2011).

For total Chl *a*, 250–400 mL seawater were filtered under low vacuum (<200 mm Hg) through 25 mm GF/F filters. These were folded and wrapped in aluminum foil or placed in Secol envelopes and stored at −80 °C or in liquid nitrogen until analysis. For size-fractionated Chl *a* (0.2–2 μm, 2–20 μm, >20 μm) 400–500 mL were filtered sequentially through 47 mm polycarbonate filters by vacuum. Filters were folded and stored in 1.5 mL cryovials at −80 °C until analysis using 90% acetone extraction by spectrofluorometric techniques on a Varian Cary Eclipse fluorometer following method APHA 10200 H (Baird, 2017)

2.3. DNA samples collection and extraction

Seawater samples of 1.5–5.0 L were filtered either through 0.22 μm filters (47 mm-diameter polyethersulfone, Pall-Gelman) using low vacuum or through 0.22 μm Sterivex filter units (Millipore) using a peristaltic pump (Cole-Palmer). Disc filters were then folded and placed in cryovials and sterivex units were filled with RNAlater and flash-frozen in liquid nitrogen prior to storing at −80 °C. Disc filters were cut in two halves first and then into small pieces using a sterile blade. Each half was placed in separate tubes and lysed in parallel (2 h at 65 °C on a Boekel thermomixer set at 750 rpm) using the Nucleospin Plant kit Midi Kit (Macherey-Nagel, Duren, Germany). The 100 μL of PL2 buffer recovered from each halved filter was then pooled together and the DNA extraction procedure continued with the Mini version of the Nucleospin Plant kit.

For Sterivex filters DNA was extracted using a Tris-buffered lysis solution containing EDTA, Triton X 100 and lysozyme (pH = 8.0) and the Qiagen DNeasy Blood & Tissue kit. Briefly, to collect cells that detached from the filter surface, the RNAlater present in the filter unit was collected into a 2 mL Eppendorf tube using a syringe and then centrifuged (13,000 rpm, 10 min). The pellet was resuspended using 1 mL of the lysis solution and pipetted back into the original Sterivex. The cartridge was sealed using Parafilm, put into a 50 mL falcon tube and incubated in a shaking incubator overnight (75 rpm, 37 °C). 1 mL of buffer Qiagen buffer AL and 40 μL of proteinase K (20 mg/mL) was then added into the Sterivex. After re-sealing the Sterivex, as described previously, the filter unit was incubated for 2 h (75 rpm, 56 °C). Following the incubations the lysate was recovered from the cartridge and DNA extraction and purification continued following the manufacturer's instructions for the Qiagen DNeasy Blood & Tissue.

2.4. PCR amplification, amplicon sequencing and sequence processing

The V4 region of the 18S rRNA gene was amplified using the eukaryotic primers TAReuk454FWD1 (CCAGCASCYGCGGTAATTCC) and V4 18S Next.Rev (ACTTTCGTTCTTGATYRATGA) with Illumina overhang adapters (TCGTCGGCAGCGTCAGATGTGTATAAGAGACAG and

GTCTCGTGGGCTCGGAGATGTGTATAAGAGACAG) (Piredda et al., 2017) and following procedures described in Gutierrez-Rodriguez et al. (2019). PCR reactions were prepared in 50 μL using 2x KAPA HifFi HotStart ReadyMix, (0.3 nM dNTP, 2.5 mM MgCl2), 0.5 μM of each primer and 30–50 ng of DNA template. The thermocycling profile included 95 °C/3 min, 10 cycles (98 °C/10 s, 44 °C/20 s, 72 °C/15 s), 15 cycles (98 °C/10 s, 62 °C/20 s, 72 °C/15 s and 72 °C/7 min). Amplicon sequencing was conducted at the Genotoul GeT core facility (Toulouse, France) using an Illumina Miseq and a 2 × 250 cycles Miseq kit version 2. 482 samples were sequenced generating a total of 9208994 reads, with a median sequencing depth across all samples of 18906 reads per sample (range = 6539–36551). Obtained sequences were processed using the DADA2 pipeline (Callahan et al., 2017) following the procedure described by Trefault et al. (2021). The default option of DADA2 (dada(..., pool=FALSE)) was used and therefore amplicon sequence variants (ASVs) only supported by more than a single read in each sample were considered. Additional thresholds to remove low abundance ASVs inferred by DADA2 were not applied.

Taxonomic assignation was conducted using the assignTaxonomy(...) function of DADA2 that implements the RDP naive Bayesian classifier method (Wang et al., 2007) against PR2 database version 4.12 (https://pr2-database.org/). We adopted the taxonomic structure of PR2 database which includes 8 levels (Kingdom/Supergroup/Division/Class /Order/Family/Genus/Species). The *classifier* method does not use sequence distance, instead the assignation is done by comparing the kmer profile of the sequences to be classified and the kmer profile generated from the reference sequence database. A bootstrapping approach is then followed to provide a measure of the confidence in the assignation for each taxonomic level including species level. In addition, we ran a BLAST against the nr database and a table with the top 20 hits for each ASVs can be found in https://github.com/agutierrez2001/Catalyst_Biogeography. For the most abundant ASVs with a low (<90) bootstrap support for species level we provided the % similarity to the closest formally identified species, and the taxonomic assignation provided by PR2 was changed if required. For other ASVs with low bootstrap support but lacking a formally described species within the top 20 BLAST hits, we raised the DADA2 assignation to the next taxonomic rank with high (>90) bootstrap support. Since the natural microvaribility within the V4 region is captured by ASV methods, and V4 sequences with very low dissimilarity annotated to the same species can be found in PR2, some ASVs were assigned to the same species.

ASVs assigned to Metazoa (13% of 18S rRNA sequences across all samples) and Fungi (0.54%) were bioinformatically removed and not considered in this study. This yielded 7,949,256 sequences and 16,861 ASVs assigned to protistan taxa. Details on the number of samples, reads and ASVs associated with each water mass are shown in (Table S1).

2.5. Pre-processing of ASV table and diversity analysis

We standardized the ASV table to the sequencing depth of each sample by normalizing the relative abundance to the mean number of sequences obtained across samples (median sequencing depth * (number of reads per ASV/total number reads per sample)). We opted for scaling the relative abundance because species richness and ordination analysis operate with species abundance (ASV counts in our case) rather than percentages. The relative contribution of specific groups in different water masses and regions were estimated from the sum of standardized reads across the samples considered. The Shannon diversity index was estimated using the plot_richness function in the phyloseq package (McMurdie and Holmes, 2013) which calls the diversity() function from the vegan R package (Oksanen et al., 2019) in its default configuration that uses the natural log.

Similarity analysis was undertaken using principal component analysis (PCA), redundancy analysis (RDA) and PERMANOVA using phyloseq (McMurdie and Holmes, 2013), microviz (Barnett et al., 2021) and vegan (Oksanen et al., 2019) R packages. Differences in species abundance across waters masses and regions was analysed using negative binomial generalized linear models coded in the DESeq2 package (Love et al., 2014).

For analysis of higher taxonomic rank (division, class), distribution and their relation to environmental variables, the tax_glom function in phyloseq was used to agglomerate the previously standardized ASV table into the chosen taxonomic level. While all protist classes were included in the analysis we focused on phytoplankton and heterotrophic and mixoplankton groups such as ciliates and radiolaria that are known to prey on phytoplankton, rather than parasitic groups like Syndiniales.

2.6. Data accessibility

Physico-chemical, biological and geographic data including measurements of temperature, salinity, oxygen and transmissivity obtained with a Seabird CTD 9plus; inorganic nutrients; total and size-fractionated chl *a*; and estimated mixed-layer and euphotic zone depth can be found in PANGAEA repository archive data sets (https://doi.pangaea.de/10.1594/PANGAEA.937633). Raw sequence data are available on NCBI under accession number PRJNA756172. The quality filtered ASV table together with the taxonomy and metadata table used to build the phyloseq object are provided as csv tables. R scripts for data processing and figures can be found in https://github.com/agutierrez2001/Catalyst_Biogeography.

3. Results

3.1. Physical, chemical and biological variability

STW was identified as those waters with surface salinity >35 psu (range = 35.1–35.6) (Fig. 2) and included samples collected during the Cross-shelf Exchange II (TAN1604), the Bay of Plenty (KAH1303), the Spring Bloom II (TAN1212) voyages, and several cruises that visited the northern mooring site (Bio-STM) of the Biophysical Moorings long-term monitoring programme (Nodder et al., 2016) (Fig. 1, Table 1 and Figure S1). The Subtropical Front (STF) had salinity values ranging between 34.4 and 35.0 psu (Fig. 2) and included samples collected during TAN1516 cruise on the Chatham Rise and the Bio-STF site during the Biophysical Mooring cruises, as well as samples collected in the S-STF during the TAN1702 cruise to the Campbell Plateau region (Fig. 1, Table 1, Figure S1). Typically SAW had salinity values <34.4 (Fig. 2) and included samples collected during the Biophysical Mooring cruises at the Bio-SAM site located in the Bounty Trough and the Campbell Plateau cruise TAN1702 that surveyed the plateau itself as well as the SAF south of the plateau (Fig. 1, Table 1, Figure S1).

Sea-surface temperature was on average lowest in SAW (10.7 ± 2.4 °C, mean ± standard deviation, sd), intermediate in the STF (13.1 ± 1.7 °C) and highest in STW (16.1 ± 3.2 °C) (Fig. 2). Temperature showed greater overlap among water masses and regions than surface salinity (Fig. 2). STW sampled during the Spring Bloom II cruise, for instance, showed surface temperature consistently lower than 15 °C (12.5–14.5 °C) (Fig. 2). Nitrate concentrations were lowest in STW (2.98 ± 1.96 μmol/L), intermediate and more variable in STF waters (4.28 ± 4.17 μmol/L) and highest in SAW (12.17 ± 4.02 μmol/L), consistent with HNLC conditions of these southern waters (Fig. 1D).

Chl *a* concentration in the surface mixed-layer was on average higher in the STF (0.65 ± 0.65 μg/L) compared to STW (0.38 ± 0.31 μg/L) and SAW (0.37 ± 0.23 μg/L) (ANOVA, $F_{2,220} = 14.2$, $p < 0.0001$) (Fig. 2). These average values were calculated from individual Chl *a* samples collected together with the DNA samples from the surface mixed layer. Results indicate that most DNA samples included in this study were taken from oligotrophic and mesotrophic waters (surface Chl *a* <0.5 μg/L) with only a few collected from waters with Chl *a* concentrations >1.0 μg/L. The smallest size-fraction (0.2–2.0-μm Chl *a*) dominated the phytoplankton communities across all water masses but

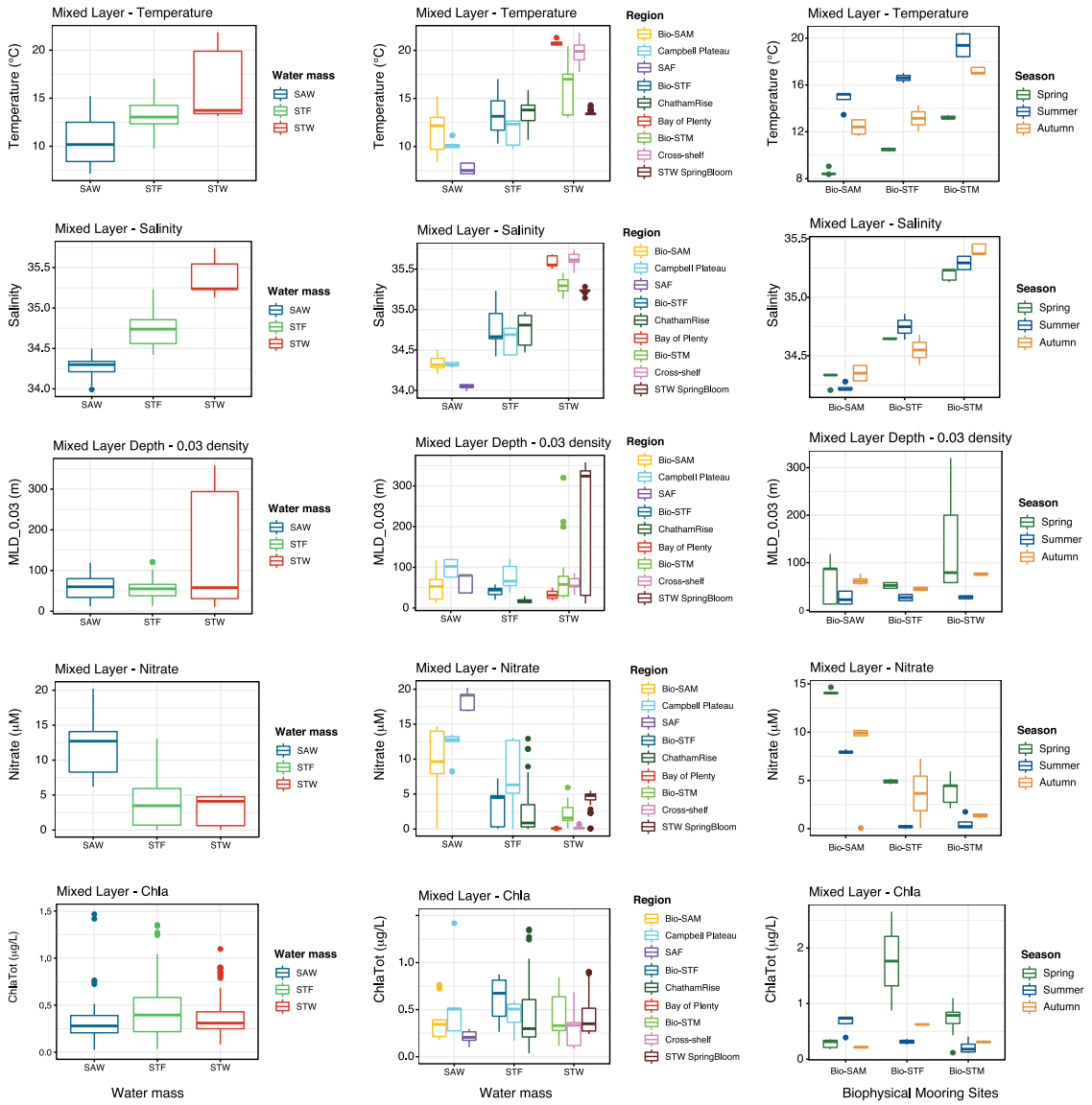

Fig. 2. Surface mixed-layer physico-chemical variability. Box-plot representation of surface mixed-layer temperature and salinity, nitrate and chlorophyll *a* concentration in each water mass (SAW, STF,STF; left panels), region (middle panels) and season (right panels). Box-plots show the median, the first and third quartiles (lower and upper hinges) and the values within the $\pm 1.5 * IQR$ (IQR, interquartile range) are represented by the line extending from the box-plot while the dots above or below are the outlier values falling outside the IQR.

more so in STW (Chl *a* <2.0 ≃ 75% of total Chl *a*) compared to SAW and STF (40%–50%, Figure S3). The contribution of >20-µm size-fraction to surface mixed layer Chl *a* was higher in SAW and STF, and although it remained on average relatively low (<15%), it occasionally reached >50% levels in these regions (Figure S3).

A more nuanced investigation revealed regional differences within each water mass (Fig. 2). In SAW for instance, SAF surface waters were colder and fresher than those on Campbell Plateau and the Bio-SAM site in the Bounty Trough (Fig. 2). Interestingly, the MLD was on average higher on Campbell Plateau than in SAW north and south of it. Surface nitrate concentrations were lower at Bio-SAM compared to Campbell Plateau and SAF, consistent with the southwards strengthening of HNLC conditions. Chl *a* concentration in the surface mixed-layer was higher on Campbell Plateau (0.62 ± 0.48, mean ± sd) compared to the Bio-SAM site (0.33 ± 0.20) and the SAF (0.21 ± 0.07) (Fig. 2), although differences were only significant between the Campbell Plateau and the SAF (one-way ANOVA, F(2, 33) = 4.494, p = 0.019).

Within STW, surface temperature and salinity were highest in northernmost waters sampled during the Cross-shelf Exchange II voyage conducted in austral late autumn (May) and lowest in STW waters sampled during the Spring Bloom II voyage conducted at the beginning of austral spring (September–October) when the MLD was highest (Fig. 2). Temperature and salinity at the Bio-STM site were intermediate on average and had a greater range, reflected also in the MLD, likely caused by the wider temporal coverage of the Biophysical-Mooring cruises (Table 1). Nitrate concentrations showed the opposite trend with highest values associated with the colder and deep-mixed waters, and lower values reflecting warmer and stratified waters of the Bay of Plenty and Cross-shelf Exchange II voyages (Fig. 2).

Regional differences were also observed in the STF, between the S-STF flowing north of the Campbell Plateau through the Snares Depression (Fig. 1), which transported colder and fresher waters, and the STF further north flowing eastwards over the Chatham Rise (STF, Chatham Rise) (Fig. 2). Nitrate concentrations tended to be higher in S-STF waters adjacent to Campbell Plateau than on the STF over the Chatham Rise reflecting the HNLC nature of the plateau. Relatively high nitrate concentrations (>10 µmol/L) were also measured at some stations of the Chatham Rise located on the southwestern flank of the STF with

colder (10.7 and 11.3 °C) and fresher (34.47 and 34.56) characteristics of surface mixed-layer waters indicating a SAW influence (Fig. 1).

Temporal variability inferred from the Biophysical Mooring sites (Bio-SAM, Bio-STF, and Bio-STM) showed canonical seasonal variability in surface temperature across the three water masses (Table 1). Conversely, temporal variability of surface salinity differed among water masses. In STW surface salinity increased from spring through summer to peak in autumn, whereas in SAW salinity was similar in spring and autumn and lowest in summer. Nitrate concentrations shared the same trend in all water masses with lowest and highest values observed during summer and spring, respectively. In STW and STF waters, Chl *a* concentrations showed a similar pattern to that of nitrate with higher Chl *a* values observed in spring. Conversely, Chl *a* concentrations in SAW were higher during summer despite nitrate concentrations being lowest during this period, consistent with the HNLC nature of these waters.

3.2. Alpha-diversity — Species richness

Species richness and the Shannon diversity index estimated in the euphotic zone were on average lower in the STF compared to SAW and STW (Fig. 3A). Highest diversity in STW was observed during the late autumn Cross-shelf Exchange II cruise and at the Bio-STM site, which included samples collected during multiple years and seasons. Protist species richness during the Spring Bloom II voyage was on average lower than at these other STW regions (Fig. 3B). In SAW diversity was lower on Campbell Plateau compared to open ocean regions Bio-SAM and SAF, adjacent to flows (Fig. 3B) located to the north and south of the plateau, respectively (Fig. 1). Within the STF, diversity was also lower in upstream waters of the S-STF located further south (46–49 °S) than in the STFZ in the Chatham Rise region (43–45 °S) (Fig. 1, Fig. 3). Here, higher diversity values were observed at the Bio-STF site located in the central region of the Chatham Rise and sampled during multiple seasons and years (Table 1) compared to the Fisheries Oceanography cruise that sampled the rise more extensively but only during one summer month (Fig. 1).

Species diversity in the euphotic zone tended to decrease with increasing latitude (model I linear regression, $F_{1,236} = 25.6$, $R^2 = 0.10$, p-value < 0.0001), although differences in mean diversity values were observed among water masses and regions at similar latitudes (Figure S4). Similar relationships were observed between diversity and temperature (model I linear regression, $F_{1,208} = 59.1$, $R^2 = 0.20$, $p < 0.0001$) with regional differences modulating this trend (Figure S5). Within STW for instance, species richness in the euphotic zone was higher in oligotrophic waters and decreased with increasing Chl *a*, being generally higher in warmer waters (Figure S6). Samples from the STF presented lower species richness in the euphotic zone compared to SAW and STW across the entire range of Chl *a* and nitrate concentrations (Figure S6).

Seasonal variability analysed at the Biophysical Moorings sites (Bio-STM, Bio-STF and Bio-SAM, $n = 56$) showed an increase in species richness from spring through summer and peaking in autumn in both STW and SAW (Fig. 3C). Only two samples per season were available for the euphotic zone at the Bio-STF site which yielded higher richness in spring than autumn with year-round minimum and maximum values estimated during summer.

Diversity patterns in the aphotic zone were investigated on the Biophysical Moorings dataset only ($n = 137$ aphotic samples). Diversity in the aphotic layer at the Bio-STM and Bio-SAM sites was lower than in the sunlit layers (Fig. 3D). In the STF, however, diversity was higher in the aphotic compared to the euphotic layer, which resulted in relatively constant species richness in the aphotic zone across different water masses unlike the diversity in the euphotic zone that showed more marked differences between sites (Fig. 3).

Table 2
Summary of PERMANOVA analysis including the Water mass and Region as categorical variables in addition to the continuous environmental variables. Temperature and salinity represent the surface values. Nitrate (NO_3^-) and chlorophyll *a* (Chl *a*) median concentration calculated for samples within the euphotic zone. Analysis was conducted with the Adonis function of the vegan R package.

Variable	Df	SumsOfSqs	MeanSqs	F.Model	R^2	Pr(>F)
Water mass	2	8.794	4.3970	24.7548	0.13564	0.001
Region	6	18.519	3.0865	17.3767	0.28565	0.001
Temperature	1	1.745	1.7446	9.8219	0.02691	0.001
Salinity	1	1.171	1.1714	6.5950	0.01807	0.001
median NO_3	1	0.991	0.9908	5.5781	0.01528	0.001
median Chl *a*	1	0.930	0.9297	5.2344	0.01434	0.001
Residuals	184	32.682	0.1776		0.50411	
Total	196	64.832			1.00000	

3.3. Beta-diversity of protistan communities

To explore the similarities between protistan communities in different geographic samples we performed principal component analysis on ASV abundance (PCA). The PCA analysis conducted with all samples yielded two main clusters corresponding to samples from the euphotic and aphotic zones (Figure S7). A subsequent RDA analysis focused on the euphotic zone clustered samples ($n = 240$) according to different water masses although certain overlaps also occurred, particularly between the STF and SAW samples (Fig. 4A). Different regions tended to cluster separately as well, with STW samples from the Spring Bloom II voyage forming a separate cluster from that of the Cross-shelf Exchange and Bay of Plenty cruises that were also conducted in STW (Fig. 4A).

To investigate the influence of different oceanographic drivers on the community composition we performed PERMANOVA analysis with continuous variables of physical (T, Sal), chemical (NO_3^- concentration – euphotic zone median nitrate and biological (Chl *a* concentration – water-column median) parameters. The analysis was conducted on a subset of samples ($n = 182$) for which these measurements were available (STW, $n = 34$, STF, $n = 53$, SAW, $n = 95$). All variables yielded statistical significance ($p < 0.001$) with salinity explaining most of the variability (F.Model = 30.3, $R^2 = 0.12$, $P < 0.001$) followed by temperature ($R^2 = 0.07$) and nitrate ($R^2 = 0.04$) with chla concentration explaining a minor fraction of this variability ($R^2 = 0.02$) (Fig. 4B) (Table S2). Overall this set of variables left 75% of the variability unexplained. The second PERMANOVA analysis included categorical variables (e.g. Water mass and region) showed that while Water mass explained 14% of the variability (F. Model = 24.7, $p < 0.001$) – similar to that explained by salinity – the region explained an additional 28% of the variability (F. Model = 17.4, $p < 0.001$) and up to 50% of the variability together with physico-chemical and biological continuous variables included in the first PERMANOVA analysis (Table 2).

3.4. Division and class level taxonomic composition in the euphotic zone

Dinoflagellata reads dominated the sequencing datasets from samples taken in the euphotic zone (51% of protist reads — sequencing depth-normalized), with relatively even partitioning between *Dinophyceae* (24%) and Syndiniales classes (27%) (Fig. 5). *Chlorophyta* accounted for 20% of reads followed by *Ochrophyta* (9%), which comprised mainly by *Bacillariophyta* (5%) and *Pelagophyceae* (2%)). Haptophytes belonging to *Prymnesiophyceae* class (5%) were the other most important phytoplankton division, while Stramenopiles_X (mainly through Marine Stramenopiles, MASTs, 4%), Radiolaria (3%), and *Ciliophora* (3%) contributed most among the heterotrophic protists. Although such groups were consistently dominant, their relative contributions and particularly, their composition at class (Fig. 5 and Fig. 6) and finer taxonomic resolution (see subsection 3.5.) varied between water masses.

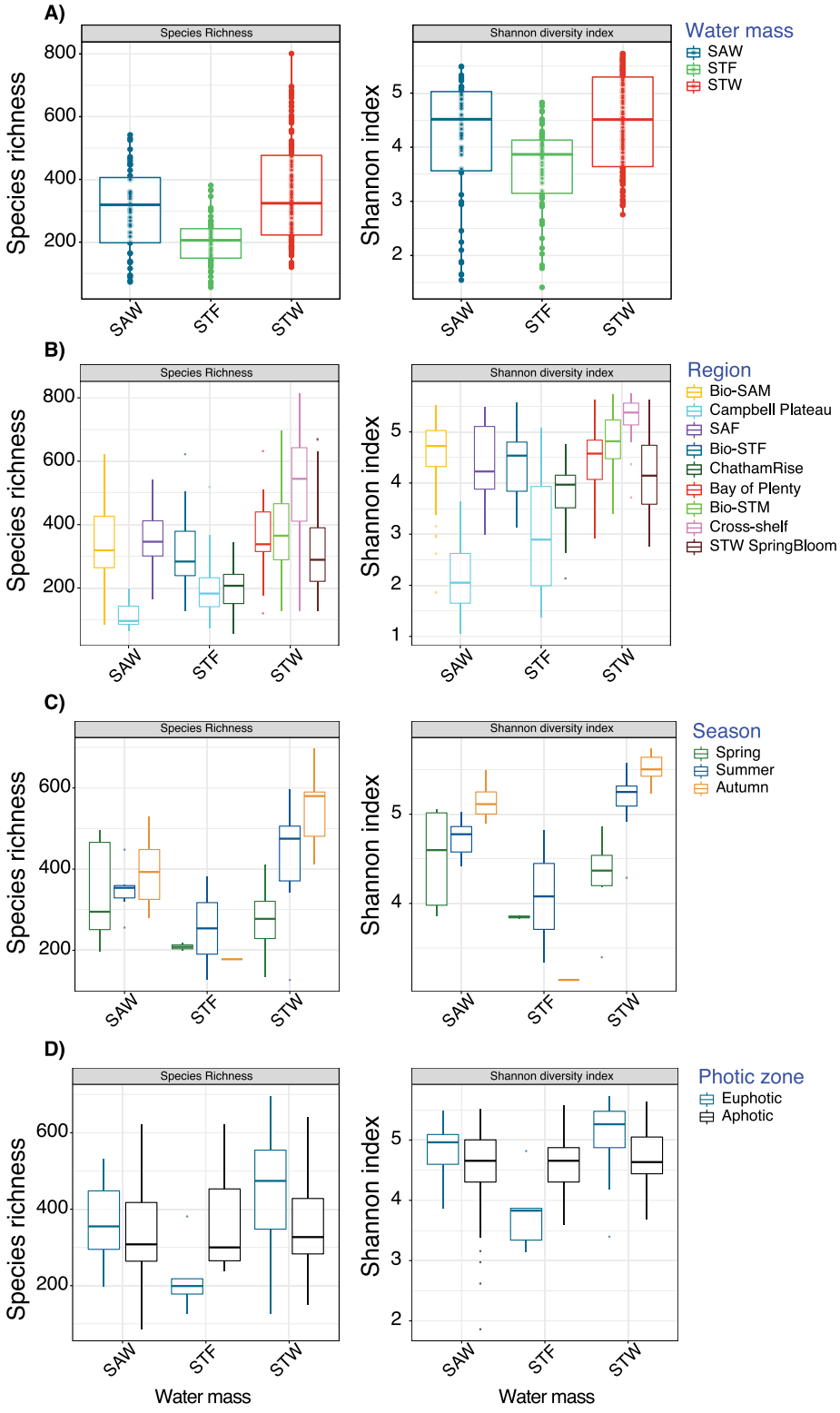

Fig. 3. Species richness and diversity index estimated for (A) the euphotic zone of each water masses (SAW, STF, and STW); (B) the euphotic zone of each region; (C) the euphotic zone in each season; (D) the euphotic and aphotic zones of the Biophysical Mooring program sites in each water mass. The Subantarctic Front (SAF) and Campbell Plateau correspond to the same voyage TAN1702 (April 2017).

For STW samples for instance, *Mamiellophyceae*, which co-dominated the community along with *Syndiniales* (24% of total protist reads each), accounted for the vast majority of reads affiliated to Chlorophyta (>95% Chlorophyta reads) while *Chloropicophyceae* represented only a minor fraction of sequences affiliated to this division (Fig. 5). *Prymnesiophyceae* was the most abundant class of Haptophyta (5%). *Bacillariophyta* (4%) and *Pelagophyceae* (2% each) classes dominated over *Dictyochophyceae* and *Chrysophyceae* (<1% *each)* among Ochrophyta,

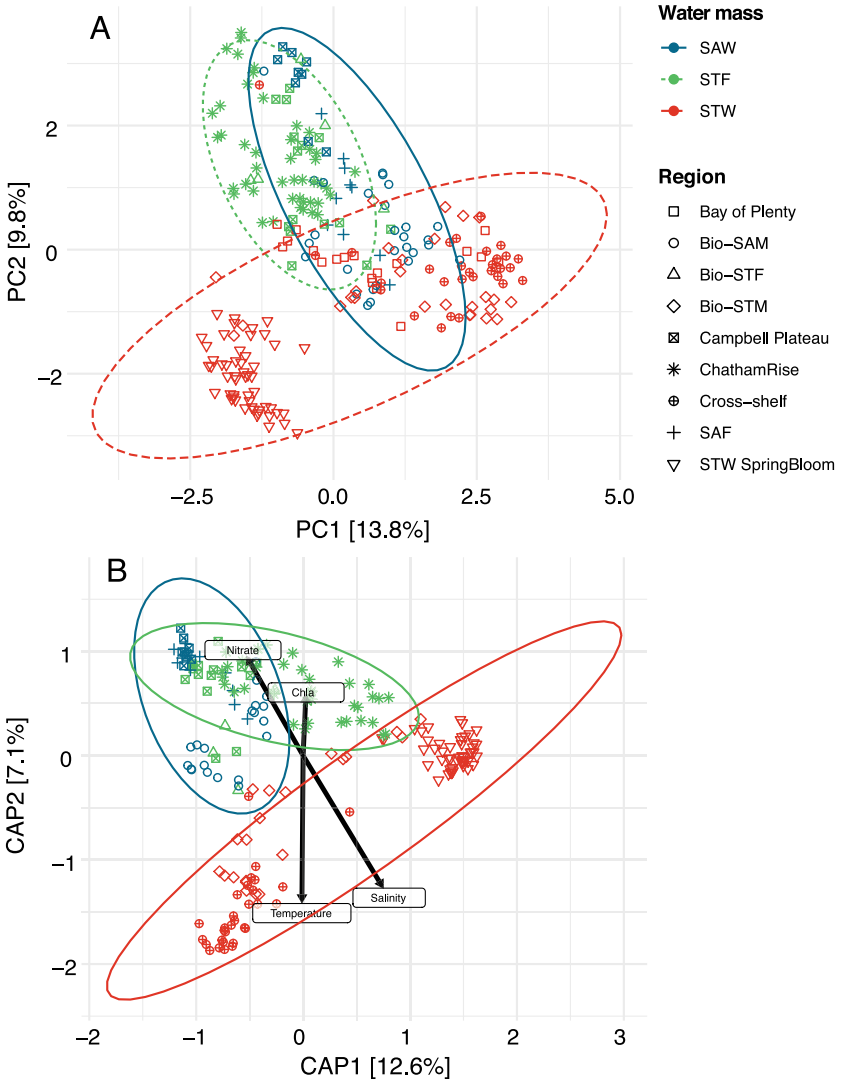

Fig. 4. (A) Principal component analysis based on ASV composition of euphotic samples colour coded by water masses and shapes for regions/voyages (n = 240). (B) Biplot of redundancy analysis computed at species (ASV) level in the euphotic zone for which T, Sal, Nitrate and Chl *a* measurements were available. Arrows indicate the sign and strength of the correlation between community composition and environmental variables that were significant in PERMANOVA analysis (n = 196). Samples from Bay of Plenty lacked Chl *a* data and were not included in the analyses.

while *Cryptophyceae* (1.2%) accounted for a slightly larger percentage on average. Among Heterotrophic groups MASTs (Stramenopile_X, 4%), ciliates *Spirotrichea* (2.2%) and RAD-A (1.4%) and RAD-B (1%) radiolarian groups contributed most to the STW metabarcoding data (Fig. 5 and Fig. 6).

The SAW sequencing dataset was clearly dominated by Syndiniales (35% total reads) and *Dinophyceae* (25% total reads) followed by *Prymnesiophyceae* (8%) and *Chloropicophyceae* (6%) (Fig. 5). Unlike STW, *Chloropicophyceae* dominated over *Mamiellophyceae* (4%) which accounted for a smaller proportion of Green algae reads. Among Ochrophyta, *Bacillariophyta* and *Pelagophyceae* phytoplankton classes showed a more even partitioning than observed in STW (4% each) (Fig. 5). The heterotrophic component in the SAW metabarcoding data was dominated by MASTs (3%) followed by *Spirotrichea* ciliates (2%) while the relative contribution of Radiolaria in the euphotic zone was minor (<1%) and mainly attributed to Polycystinea (0.5%) rather than RAD-A and -B classes (0.2%) (Fig. 5 and Fig. 6).

The STF protist metabarcoding data presented intermediate characteristics between STW and SAW (Fig. 5). As in SAW, Dinophyceae (30%) and Syndiniales (27%) co-dominated the metabarcoding dataset. The contribution of Chlorophyta (17%) was, however, higher and closer to levels found in the STW metabarcode dataset. Accordingly, *Mamiellophyceae* was the most abundant class of green algae (12%), with *Chloropicophyceae* (4%), and *Pyramimonadophyceae* (1.5%) having lower but still substantial relative abundances. The division Ochrophyta (10%) accounted for a similar fraction of phytoplankton reads as in STW and SAW, but in STF the phytoplankton community was clearly dominated by *Bacillariophyta* (8%) with minor contributions from *Pelagophyceae* (1%) and *Dictyochophyceae* (0.3%) classes. The heterotrophic component was dominated by MASTs and *Spirotrichea* ciliates (3% each) while the contribution of Radiolaria (<0.2%) was on average lower than in STW and SAW datasets and dominated by RAD-A and RAD-B lineages (Fig. 5 and Fig. 6).

Temporal variability analysed from the Biophysical moorings dataset showed an increase in the relative contribution of *Mamiellophyceae* during spring at both Bio-STM and Bio-SAM sites. At the Bio-STM site, diatoms accounted for a substantial proportion of protist reads in the surface mixed-layer during the TAN1113 spring voyage, while they peaked in subsurface waters during the TAN0902 summer voyages (Fig. 7). Diatom contributions at the Bio-SAM site was also higher in spring and summer compared to autumn, although their overall contribution remained lower than in the Bio-STM site. Dinoflagellate contributions remained fairly constant through time at both Bio-STM and Bio-SAM sites. Prymnesiophytes tended to be

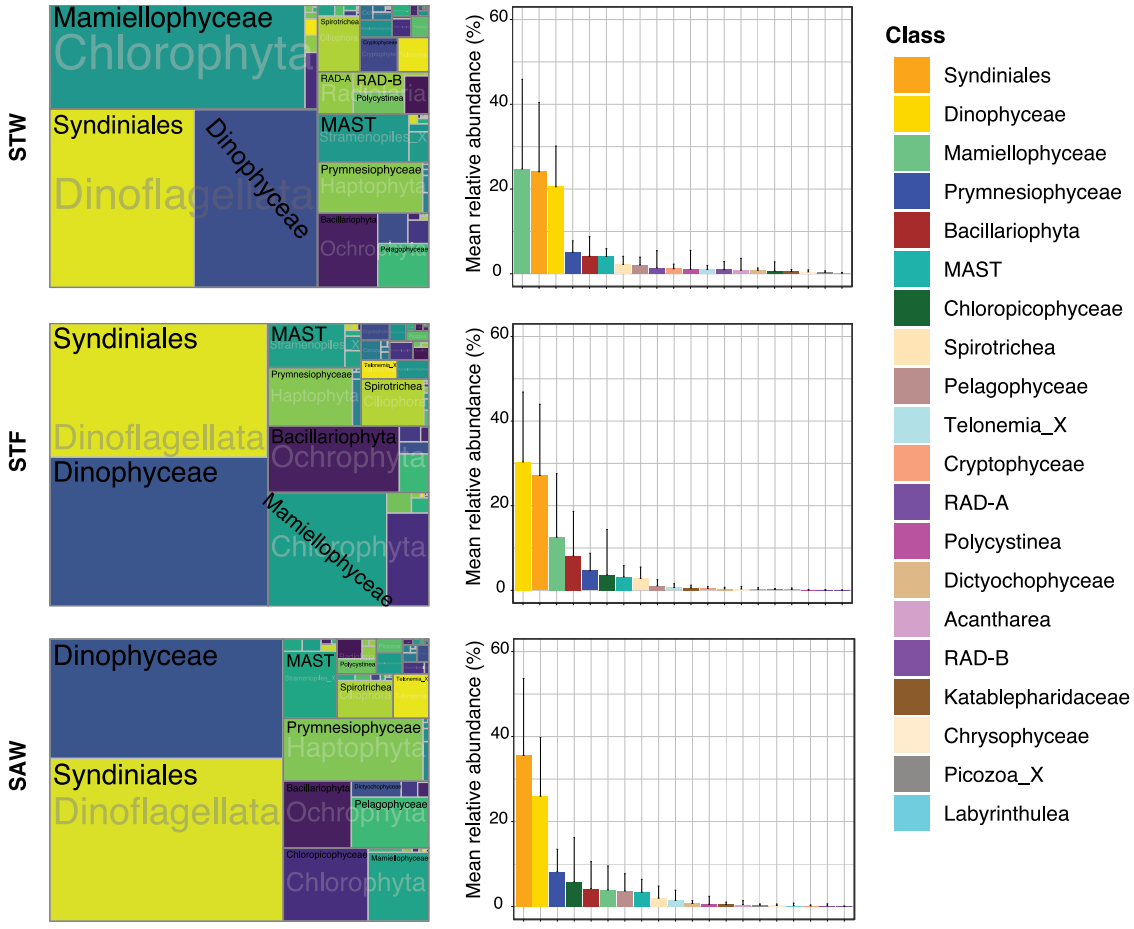

Fig. 5. Treemaps showing the taxonomic composition at division/class level of the protistan communities in the euphotic zone of Subtropical (STW), Subtropical Front (STF) and Subantarctic (SAW). The area of each taxonomic group in the treemap represents the read abundances affiliated to each group standardized to the median sequencing depth across samples [median sum ASVs * (ASV reads/sum (ASV reads)]. The barplots represent the mean relative read abundance of most abundant classes across different water masses (error bars are the standard deviation of the mean).

more abundant during summer in Bio-STM while they showed similar relative abundances across all three seasons at the Bio-SAM site. The highest relative abundance of pelagophytes were observed at Bio-SAM during summer and autumn in SAW, with no clear pattern observed at Bio-STM where the contribution of this group tended to be lower (Fig. 7).

To investigate protist community composition below the euphotic zone we also used the Bio-physical moorings dataset, which covered systematically the entire water column at the Bio-STM and Bio-SAM (0–3100 and 0–2800 m, respectively) sites and the Bio-STF site on the Chatham Rise crest (0–350 m) (n = 137 aphotic samples). Overall, Dinoflagellates dominated the metabarcode dataset mainly through Syndiniales (40 ± 15%) which contributed substantially more than Dinophyceae (14 ± 10%). Radiolaria was the second most abundant group accounting for a third of metabarcodes on average (31 ± 20%) (Figure S8). Among Radiolaria, the Polycystinea class, mainly through the Spumellaria, was most abundant (21%), although Acantharea (6%), RAD-B (4%) and to a lesser extent RAD-A (0.7%) classes also contributed to the dominance of this group (Fig. 7 and Figure S8). The contribution of both Radiolaria and Syndiniales was on average lower in the STF, where Dinophyceae relative abundance peaked, compared to STW and SAW. All three classes contributed similarly in the aphotic zones of STW and SAW (Figure S8). Other heterotrophic groups such as MASTs (1.5%) and ciliates (1%), contributed less but showed the same pattern with 2-fold higher relative abundance in STF (3% and 1.5%) compared to STW and SAW (1–1.5% and 0.6%–1%). (Fig. 7 and Figure S8). Among phytoplankton groups, diatoms, green algae, and prymnesiophytes were most abundant and contributed at similar levels (1.0–1.5% each), likely reflecting deep mixing layers extending below the euphotic zone (Fig. 7 and Figure S8).

Vertically, the dominance of Radiolaria became more prominent in the mesopelagic and bathypelagic samples where they often represented up to 50% of total reads (Fig. 7). Polycystinea class tended to dominate across all sample depths, with increasing abundance at depths >300 m. Sequences affiliated with Acantharea and RAD-B showed similar abundances but followed opposite vertical distributional trends, with RAD-B being more abundant in shallower samples (100–500 m) while Acantharea abundance increased with depth and peaked in bathypelagic samples (>1000 m) (Fig. 7).

3.5. Genus and species community composition

Species composition also varied among the metabarcodes from the physically and biogeochemically distinct water masses (Fig. 8, Figure S10). In STW, the green algae (Chlorophyta) was dominated by *Ostreococcus* sp. (ASV_0001) followed by *Bathycoccus prasinos* (ASV_0006). These *Mamiellophyceae* species together with *Micromonas commoda* (ASV_0013) and other *Micromonas* species (*M. pusilla* (ASV_0031, ASV_0074) and *M. bravo* (ASV_0062)) and accounted for the majority of the sequences affiliated to green algae in the euphotic zone of STW (Fig. 8, Figure S9 and Figure S11). Among the most abundant dinoflagellates in STW we found several ASVs belonging to *Gymnodiniales* and *Gyrodinium* spp., and unidentified ASV_0010 most closely related to *Ptychodiscus noctiluca*. *Gymnodinium* spp., were more abundant at Bio-STM whereas unidentified ASV belonging to Syndiniales

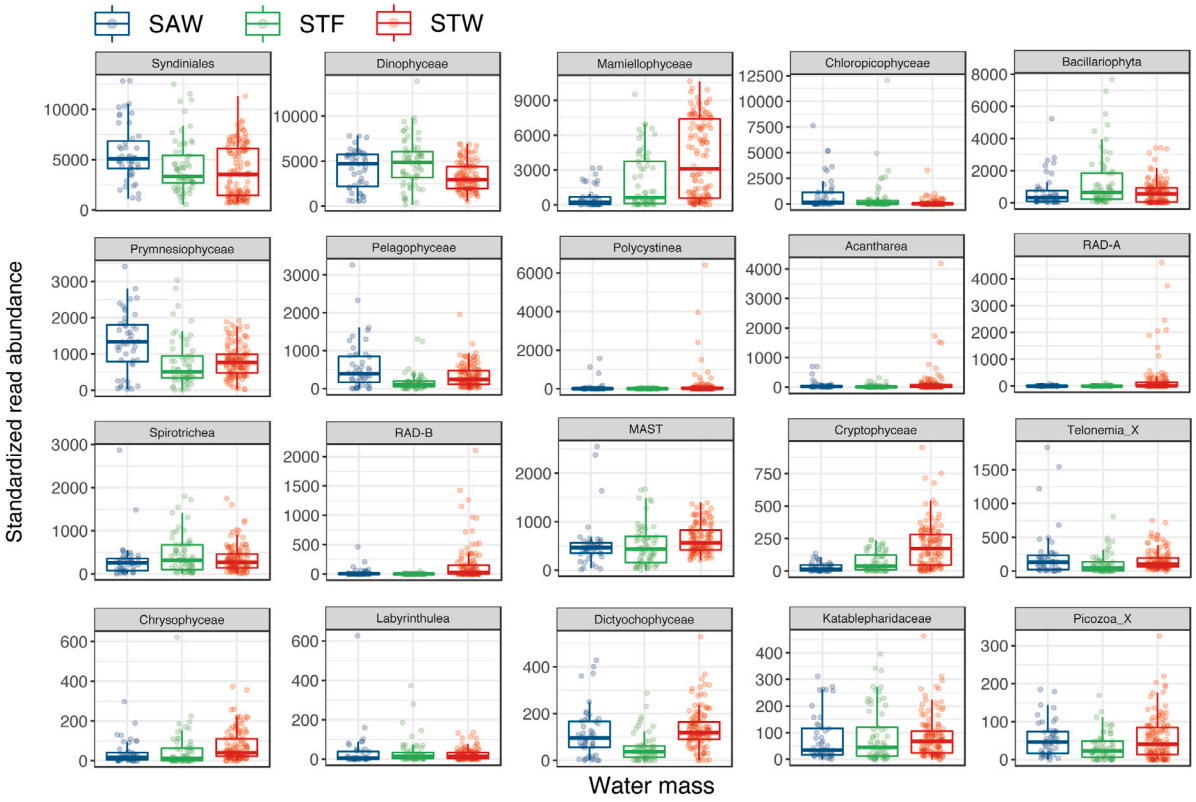

Fig. 6. Box-plots showing standardized read abundance in the euphotic zones of subtropical (STW), Subtropical Front (STF) and subantarctic (SAW) water masses of the twentieth most abundant protist classes. Box-plots show the median, the first and third quartiles (lower and upper hinges) and the values within the $\pm 1.5 * IQR$ (IQR, interquartile range) (line). Points represent values of single samples.

Group-II (ASV_0002) and *Gyrodinium* sp. (ASV_0256) emerged also as a prevalent species during the Cross-shelf Exchange voyage (Figure S11). Diatom ASVs belonging to Polar-centric *Mediophyceae*, identified as *Brockmanniella brockmanii* (ASV_0030) and *Minidiscus trioculatus* (ASV_0042), were the most abundant diatom reads in STW metabarcodes, particularly during the Spring Bloom II voyage. Diatom ASVs belonging to Radial-centric diatoms in class Coscinodiscophyceae identified as *Guinardia* sp. (ASV_0443, 100%) became regionally abundant at the Bio-STM site. Among ASVs assigned to pelagophytes, *Pelagomonas calceolata* (ASV_0044) and unidentified Pelagophyceae_XXX_sp. (ASV_0058) with closest reference to *Aureococcus anophagefferens* (99.6% similarity) were the most abundant ASVs (Fig. 8, Figure S11 and Figure S9). Among the class *Prymnesiophyceae*, *Phaeocystis globosa* (ASV_0065) was the most abundant ASV (Fig. 8).

Among the STF metabarcodes, ASVs assigned to Syndiniales Group-I (ASV_0002, ASV_0022) were the most abundant ASVs (Fig. 8). Mamiellophyceae *Ostreococcus* sp. was also among the most abundant species overall, although the relative contribution of several *Chloropicophyceae* ASVs identified as *Chloroparvula pacifica* (ASV_0014) or most closely related to this species (ASV_0086, 99.7% and ASV_0336, 99.5%) increased substantially compared to STW (Fig. 8, Figure S9). It is worth noting the high abundance of sequences affiliated to *Chloropicon* sp. in addition to *Chloroparvula pacifica*, which contributed to the overall increase in the relative abundance of *Chloropicophyceae* in the STF dataset (Fig. 8, Figure S9). ASVs assigned to the heterotrophic dinoflagellate *Gyrodinium* sp. were among the most abundant in STF samples, with other ASVs affiliated with *Warnowia* sp. and *Karlodinium* sp. dinoflagellate species becoming prevalent as well (Fig. 8, Figure S10 and Figure S9). The higher relative abundance of Bacillariophyta observed in STF was mainly driven by ASVs affiliated to Polar-centric *Mediophyceae* species such as *Minutocellus polymorphus* (ASV_0100), *Brockmanniella brockmanii* (ASV_0030), *Fragilariopsis* sp. (ASV_0036), which was most closely related to *F. sublineata* (99.3%). In addition to Polar-centric species, ASVs assigned to *Thalassiosira* sp. (ASV_0093), *Cerataulina pelagica* (ASV_0202), *Leptocylindrus* sp. (ASV_0581), and several unidentified diatom species also emerged among the most abundant diatom species in the Chatham Rise region (Fig. 8 and Figure S11). The identification of *F. sublineata* should be taken with caution because the V4 region of the two sequences included in PR2 is 100% similar to the annotated sequence of *Fragilariopsis kerguelensis*, making it impossible to unambiguously assign the ASVs identified as *Fragilariopsis* sp. to *F. sublineata* or *F. kerguelensis* species. To reflect this ambiguity the ASVs assigned to *F. sublineata* in PR2 are referred as *F. sublineata/kerguelensis* throughout the text (see discussion). Among *Prymnesiophyceae*, *Phaeocystis antarctica* (ASV_0027, ASV_0179) was the most abundant species instead of the *P. globosa* found in STW. ASV_053 coccolithophore having 100% similarity with *Emiliania huxleyii* and *Reticulofenestra parvula* increased substantially relative to STW dataset, particularly in the Chatham Rise region (Fig. 8, Figure S11). *Pelagophyceae* in the STF metabarcodes was dominated by *Aureococcus* and *Pelagococcus* spp. (Figure S9) although the overall relative contribution of *Pelagophyceae* was relatively low (Fig. 5). The relative abundance of *Cryptophyceae* and *Dictyochophyceae* remained minor overall (<2%) (Fig. 5), but both groups showed changes in their specific composition across the water masses metabarcode datasets. Among *Cryptophyceae*, ASVs identified as *Plagioselmis prolonga* (ASV_0102) and *Teleaulax* sp. (ASV_0107) increased substantially from STW to STF samples at the cost of the decrease of ASV assigned to *Geminigera* sp. (ASV_0174) which was closely related (99.5%) to partial V4 sequence of *Geminigera cryophila* RCC5152 strain. *Plagioselmis prolonga* (ASV_102) clearly dominated SAW waters where the contribution of ASVs assigned to *Teleaulax* sp. was lowest (Figure S9). Changes within *Dictyophyceae* were less substantial but showed an increase in the relative abundance of ASVs assigned to *Dictyocha* sp. and *Pseudochattonella* sp. from STW to STF metabarcodes (Figure S9).

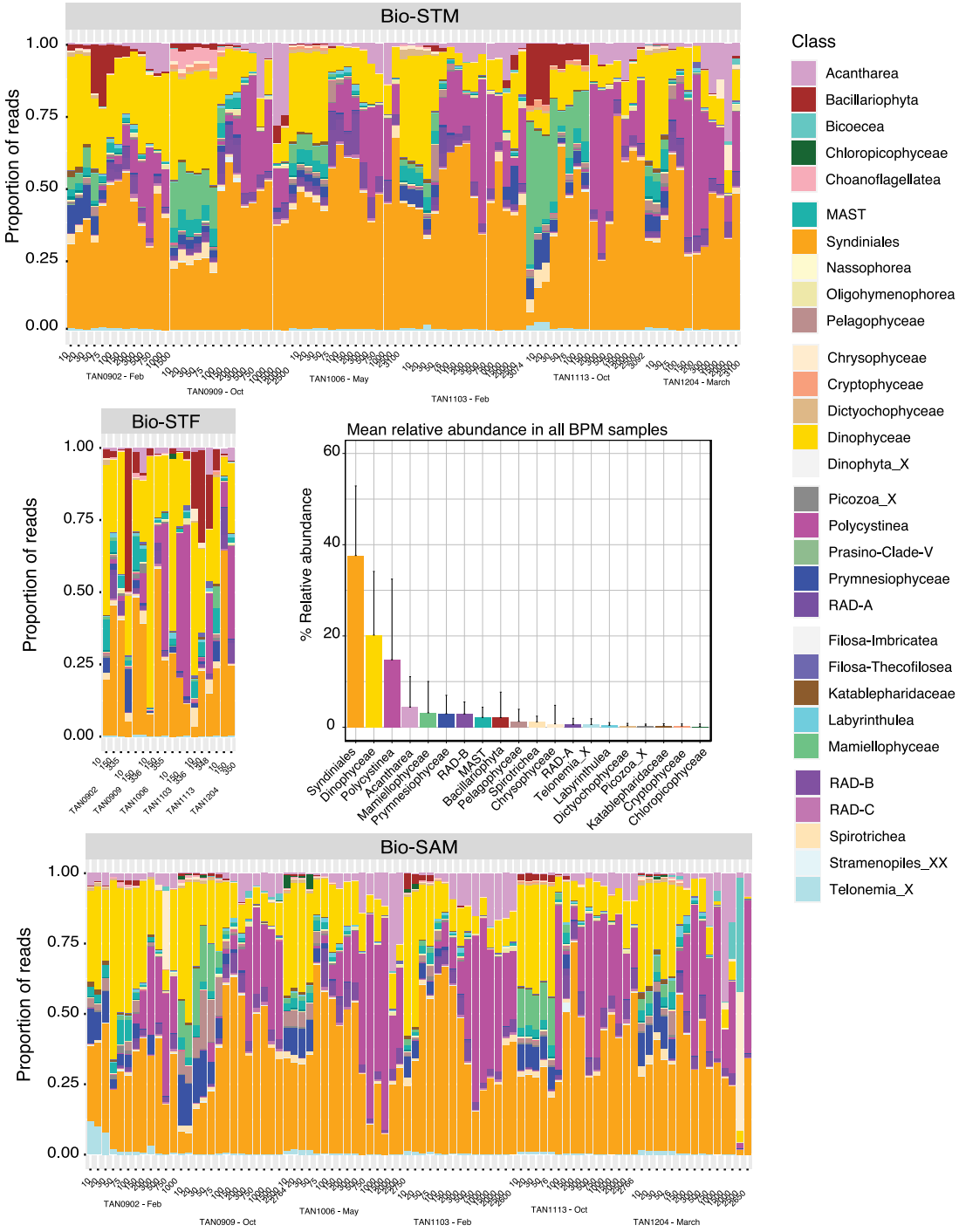

Fig. 7. Relative read abundance of main protistan classes in samples collected at different depths during multiple voyages during the Biophysical Moorings (BPM) program at Bio-STM, Bio-STF, and Bio-SAM sites. Numbering and text on the *x*-axis indicate the cruise name, month and sampling depths. Mean relative contribution of main classes averaged for the whole sampling programme are also shown (n = 193) (error bars as in Fig. 4.).

Among SAW samples, ASV_0002 belonging to Syndiniales Group-I was the most abundant taxa followed by *Fragilariopsis sublineata/kerguelensis* and *Chloroparvula pacifica*. ASV_0014 was again the most abundant strain of *Chloroparvula pacifica*, with other ASVs of this species (e.g., ASV_0086) contributing also to the dominance of *Chloropicophyceae* over *Mamiellophyceae* in SAW (Fig. 8, Figure S10, Figure S11). Among *Mamiellophyceae*, *B. prasinos* (ASV_0006) was present also in STW and STF waters and became the dominant species followed by *M. commoda* while the contribution of *Ostreococcus* sp. in SAW samples was minor (Fig. 8 and Figure S11). The increase in the relative abundance of *Prymnesiophyceae* reads observed in SAW samples was driven mainly by ASVs belonging to *P. antarctica* with ASV_0024 rather than ASV_0179 emerging as the most abundant ASV in SAW metabarcodes (Fig. 8). ASVs identified as *P. globosa* (ASV_0177) and *P. cordata* contributed also to the dominance of *Phaeocystis* spp. within this class (Figure S9 and Figure S11). Among Bacillariophyta, ASVs assigned to *F. sublineata/kerguelensis* (ASVs 0061 and 0036) were dominant in SAW samples (Fig. 8 and Figure S10) while Polar-centric Mediophyceae species like *Minutocellus polymorphus* were among the most abundant ASVs only on Campbell Plateau Figure S11). Increasing abundance of pelagophyte reads in SAW was due to *Pelagophyceae*_XXX_sp (ASV_0081) most closely related to *Aureococcus*

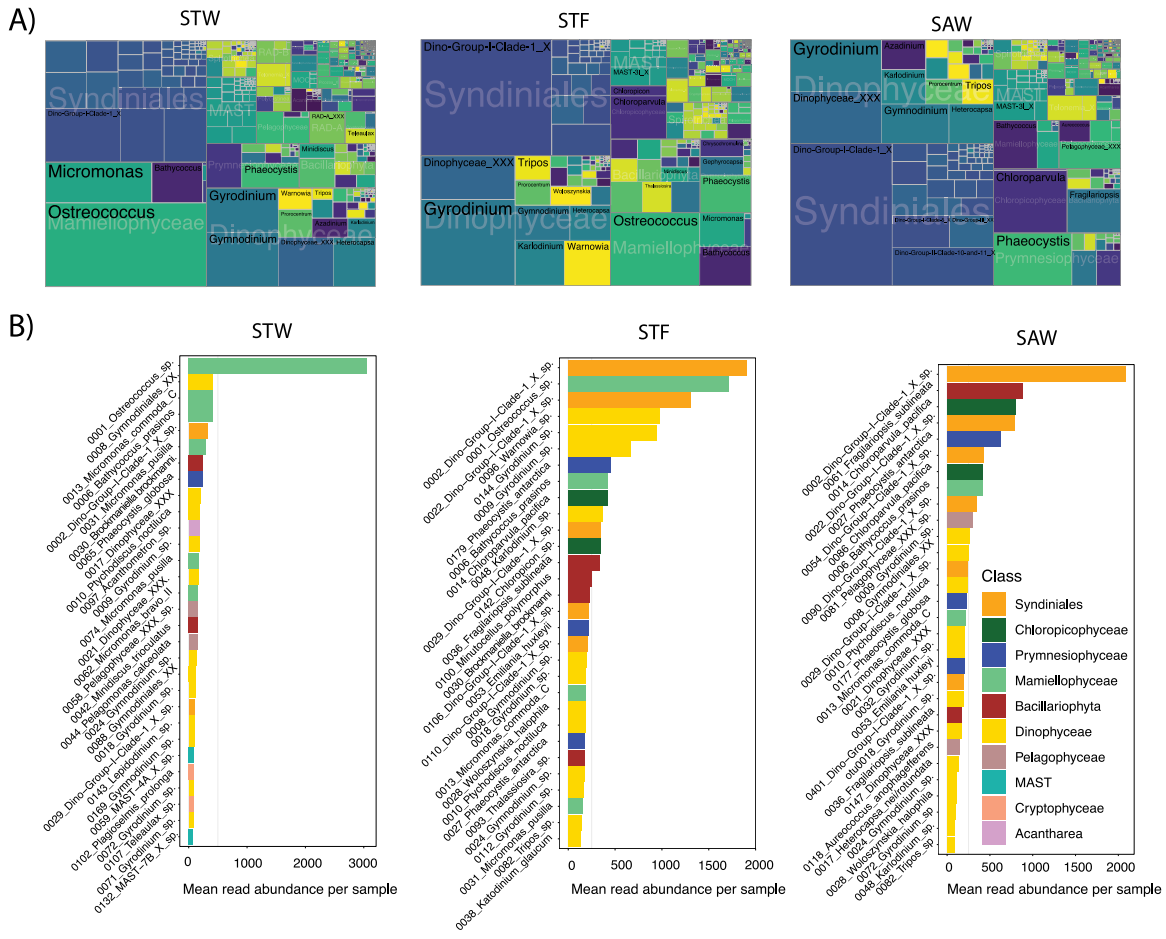

Fig. 8. Water mass genus and species abundance (A, Top panels) Treemaps showing the community composition at class/genus level in the euphotic zones of the subtropical (STW), Subtropical Front (STF) and subantarctic (SAW) water masses. The area of taxonomic group is proportional to the read abundances affiliated to each group standardized to the median sequencing depth across samples [median sum ASVs * (ASV reads/sum (ASV reads)]. (B, Bottom panels) Mean standardized read abundance of most abundant ASVs and assigned species, colour coded for their class affiliation, in the euphotic zone of the different water masses.

sp. clone from the Beaufort Sea (99.6%), and ASV_0118) identified as *Aureococcus anophagefferens* (Fig. 8 and Figure S9). The contribution of *Cryptophyceae* in SAW was very low (0.18 ± 021%) but unlike STW, *Plagioselmis* sp. clearly dominated accounting for >85% of the sequences affiliated to this class (Figure S9).

To investigate how the relative abundance of different species and ASVs varied between water masses, we ran a differential gene expression analysis based on the negative binomial distribution (DESeq) using water mass as a categorical variable. For the euphotic zone, this yielded 70 and 35 ASVs out of 3984 ASVs that were significantly more or less abundant (p-value <0.01) in STW compared to SAW datasets, respectively (Figure S12A). ASVs that showed greatest differences (>ten log2-fold changes) in their relative abundance were not necessarily among the most abundant ones in each water mass. Among the species associated with STW, we found the largest changes in relative abundance in the diatom ASVs assigned to Polar-centric Mediophyceae, *Minutocellus polymorphus*, and *Minidiscus trioculatus*; the prasinophytes *Ostreococcus* sp. and *Micromonas* spp.; the prymnesiophytes *Phaeocystis globosa* and *Chrysochromulina* sp., and the dinoflagellate ASVs assigned to *Warnovia* sp. and *H. rotundata* (Figure S12). Among species with preferences for SAW we found several diatom ASVs including those identified as *F. sublineata/kerguelensis* and most closely related to *Cylindrotheca closterium* (99.5%), the prasinophyte ASV *B. prasinos*, the pelagophytes ASVs identified as *Pelagococcus* sp. and *A. anophagefferens*, and several dinoflagellates including the ASVs belonging to heterotrophic *Gyrodinium* sp. and mixotrophic *Karlodinium* sp. (Figure S12).

Different ASVs affiliated to the same species often showed distinct preferences for STW and SAW. Most abundant *Chloroparvula pacifica* ASVs (e.g. asv_0014 and asv_0086, Fig. 8), identical or having one mismatch to indexed cultures of *Chloroparvula pacifica* were associated with SAW, while less abundant ASVs (e.g. ASV_0532 and ASV_0336) that had 2–3 mismatches with culture isolates, showed preference for STW (Figure S12A). Similarly, most abundant ASVs of *P. antarctica* (ASV_0011, ASV_0027) were distinctively associated with SAW (10 to 30 log2 fold negative changes) while much less abundant ASV_0218 showed greater affinity for STW. This strain variability was observed also within species with more uncertainties in the species level assignation (e.g. *Dinophyceae*_XXX_sp. and *Pelagophyceae*_XXX_sp.) suggesting the opposite affinities for STW and SAW observed for ASVs within these groups could reflect different ecological preferences at the species rather than strain level (Figure S12A).

DESeq analysis between the STF and STW also depicted specific differences as observed between STW and SAW, with some additional diatoms ASVs assigned to *Thalassiosira* sp. and *Pseudo-nitzschia delicatissima* enriched in the STF dataset (Figure S12B). In most cases, the distinctive species pattern observed between the STF and either STW or SAW metabarcodes coincided with those identified from the comparison between STW and SAW described above (Figure S12B). For instance, ASVs belonging to Polar-centric Mediophyceae species found in higher abundance in STW compared to SAW, were also associated preferentially with STF compared to SAW while diatoms ASVs identified as *F. sublineata/kerguelensis*, and *Cylindrotheca closterium* that were enriched in SAW compared to STW, were also preferentially associated

with the STF rather than STW (Figure S12B). Only few ASVs, such as those assigned to the prasinophyte *Chloropicon* sp. and dinoflagellate *Gonyaulax* sp., were distinctively associated with STF waters (Figure S12C).

The most abundant reads found below the euphotic zone belong to the Syndiniales Group II and the polycystinean order Spumellaria Group I family (Figure S8). Several ASVs contributed to the dominance of Spumellaria Group I family, but different ASVs dominated in each water mass dataset (Figure S13 and Figure S14). ASV_0023 and ASV_0039 affiliated with the Group I family of Spumellaria dominated in SAW, while ASV_0064 and ASV_0085 were most abundant in STF (Figure S14). Conversely, most abundant radiolarian species in STW were unidentified species assigned to the acantharean order Chauncanthida (Figure S14). Several less abundant Radiolaria ASVs showed significantly different abundances across the aphotic depth layers of different water masses suggesting differences in their ecological preferences (Figure S15). Reads assigned to known photosynthetic species also showed differential abundance below the euphotic zone in the different water masses datasets. Most notably the higher abundance of reads affiliated to the *Mamiellophyceae Ostreococcus* sp. and the *Prymnesiophyceae P. globose* in STW compared to SAW yielded significant differences in their abundance below the euphotic zone as well. A pattern also observed for less prominent diatoms ASV_0480 and ASV_0291 identified as *Asterionellopsis glacialis* or *Thalassiosira rotula*, respectively, that despite being less abundant in the euphotic zone yielded significant differences in their abundances below the euphotic zone.

4. Discussion

The taxonomic composition of protistan communities in SAW and STW in the SW Pacific and across the main frontal zones of the region (STF, SAF) has not been extensively characterized. Previous studies have typically focused on phytoplankton communities and their variability across SAW and STW flanking the STF zone over the Chatham Rise (Chang and Gall, 1998; Hall et al., 2001; Delizo et al., 2007) but broader biogeographic studies in the SW Pacific are scarce (DiTullio et al., 2003). By using DNA metabarcoding, we provide a comprehensive taxonomic characterization of the protistan communities associated with STW and SAW at southern temperate latitudes. Although samples included in this study were collected in different seasons, the seasonal coverage was similar for STW and SAW (Table 1 and Figure S1), allowing a meaningful comparison among the microbial communities associated with these water masses throughout an average year. Analysing the seasonal variability was beyond the scope of this study, since the bulk of the dataset was collected from different regions and times of the year. Only samples collected as part of the Biophysical Mooring time-series provided an adequate framework to evaluate seasonal variability. However, since the number of time points obtained for these sites (Bio-SAM, Bio-STF, and Bio-STM) was rather limited (2 time points per season for spring, summer, and autumn), we only briefly discuss the influence that seasonality may have on water mass and regional patterns presented in this study.

4.1. Protistan community structure in STW and SAW of the southwest Pacific

Species richness decreased latitudinally and with temperature (Figure S4 and Figure S5) as expected from global diversity patterns observed and modelled for marine bacterial and phytoplankton communities (Fuhrman et al., 2008; Barton et al., 2010; Ibarbalz et al., 2019) as well as from previous DNA-based reports in the SW Pacific region (Raes et al., 2018). Consistent with this trend, species richness was higher in warmer STW than in SAW while lowest diversity was associated with the STF (Fig. 3).

The relative low diversity observed in the STF could be related to the physically dynamic nature of the STFZ over the Chatham Rise (Sutton, 2001; Chiswell, 2013), the increased phytoplankton biomass and productivity typically associated with the STF across the annual cycle (Murphy et al., 2001; Pinkerton et al., 2005), and the dominance of fewer 'bloom-forming' species in this highly productive zone (Chang and Gall, 1998). The fact that species richness within STW was lowest during the more productive spring bloom conditions surveyed in STW during the TAN1212 cruise is consistent with the view that more productive waters such as found in the STF, and locally on the Campbell Plateau (Gutiérrez-Rodríguez et al., 2020) tend to decrease protistan diversity. The lower diversity observed during Spring, particularly in the Bio-STW site further support this view (Fig. 2). However, the lower diversity associated with STF, relative to STW and SAW, was systematically observed across the different levels of nitrate and Chl *a* concentrations encompassed in this study (Figure S6) suggesting that other factors may contribute to this pattern. Interestingly, the lower diversity in the STF relative to STW and SAW was buffered below the euphotic zone (Fig. 3C). The lower abundance of protists at depth (Pernice et al., 2015) could contribute to the lower diversity obtained in the aphotic zone with similar sampling effort (e.g. 4–8 L filtered seawater) to that applied to the euphotic zone. While we cannot completely rule out this possibility, the fact that the species richness we found in the aphotic zone was similar to that obtained with >10-times sampling volumes (100 L) in the bathypelagic zone across the globe (Pernice et al., 2016) supports the ecological significance of the different spatial patterns we found between the aphotic and euphotic zones. Similarly, the temperature-driven latitudinal pattern described globally for epipelagic plankton also disappeared below the euphotic zone (Ibarbalz et al., 2019). The decoupling between the diversity patterns in the sunlit and dark ocean suggested by these results are somewhat contrary to the connectivity between the epi- and bathypelagic zones as inferred by the high correspondence of bacterial communities and processes between these realms (Mestre et al., 2018; Ruiz-Gonzalez et al., 2020). The reasons for these differences are unclear and highlight the need of further study of the ecological processes that shape microbial diversity throughout the entire water column.

Despite the regional and seasonal variability encompassed within both STW and SAW (Table 1, Fig. 2) we observed systematic differences in the taxonomic composition associated with these water masses (Fig. 4). Such water-mass specificity has been previously observed for the prokaryotic (Galand et al., 2010; Agogué et al., 2011; Seymour et al., 2012; Techtmann et al., 2015) and eukaryotic components (Hamilton et al., 2008; Raes et al., 2018) of microbial communities across different oceans. Among environmental drivers, salinity rather than temperature or nitrate concentration was the physico-chemical variable that explained best the compositional (dis-)similarities among euphotic samples in the present study (Fig. 4, Figure S7). Bray–Curtis dissimilarity indices of surface bacterial communities across the Southland Current was also strongly correlated with salinity (Baltar et al., 2016). These results support the view that STW and SAW east of New Zealand are better conceptualized as bioregions or provinces, where (phyto)plankton communities reflect oceanographic processes and history in addition to contemporary physico-chemical conditions, rather than habitats (sensu Martiny et al., 2006).

Samples from the STF itself were also distinguished from those in SAW and STW based on their taxonomic composition, although they showed a greater overlap (Fig. 4) that reflected the active mixing and transition nature of such frontal zones. This overlap was particularly evident between samples collected at the Bio-STF and Bio-SAM sites located on the Chatham Rise and its subantarctic flank, respectively, and between the S-STF and SAW over the Campbell Plateau, which suggests a stronger physical connectivity and ecological affinity of the STF with SAW than STW. Similarly, the horizontal mixing and phytoplankton community size structure in the STF zone has been

reported to be more tightly coupled across SAW-influenced than STW-influenced water types (Safi et al. submitted). Nevertheless, the distinct protistan communities observed in STW and SAW, and to a lesser degree in the STF, highlight the role of oceanographic features such as the STF as boundaries that influence the diversity of oceanic microbial communities in large oceanic provinces (Baltar et al., 2016; Raes et al., 2018).

4.2. Taxonomic composition of phytoplankton community

Our results showed the overall dominance of dinoflagellates and Chlorophyta across all water masses, followed by Bacillariophyta, *Prymnesiophyceae* and *Pelagophyceae* (Fig. 5). Yet consistent differences in the relative contribution of these taxonomic groups between water masses emerged at finer taxonomic classification levels (Fig. 6, Fig. 8, Figure S9). Analysis of intra-specific diversity revealed differences in the distribution of ASVs of the same species suggesting the presence of different ecotypes in some cases (e.g. *Chloroparvula pacifica*, *P. antarctica*) and current taxonomic gaps within certain groups that remain to be characterized (e.g. *Pelagophyceae*; *Dinophyceae*) (Figure S12). Below we discuss the distributional patterns of major taxonomic groups, highlighting different taxonomic ranks to shed some light on their ecological preferences.

4.2.1. Chlorophyta (Green algae)

The relative contribution of the two main green algae classes, *Mamiellophyceae* and *Chloropicophyceae*, showed opposite distribution patterns with higher contributions in STW and SAW, respectively (Fig. 5, Fig. 6). Picoplanktonic alga *Ostreococcus* sp. was clearly the most abundant species in STW and STF (Fig. 8, Figure S10) in agreement with previous metabarcoding analysis conducted across the nearby Southland Current, a coastal expression of the STF (Allen et al., 2020), and in coastal waters globally (Tragin and Vaulot, 2019).

The dominance of picoplanktonic *Mamiellophyceae* in STW is consistent with the greater contribution of <2 μm Chl *a* (80%,) observed in this water mass (Figure S4). The highest abundance of this group was observed during the onset of the spring bloom samples (TAN1212, Figure S11) when *Mamiellophyceae* accounted for 40%–75% of 18S rRNA reads (Figure S16). Among the multiple surveys of the Bio-STM and Bio-SAM sites, *Mamiellophyceae* contributions tended to be highest during early spring coinciding with the onset of the spring bloom (Fig. 7). *Mamiellophyceae* and *Ostreococcus* sp. were the most abundant phytoplankton class and species in the STFZ over the Chatham Rise (Figure S16 and Figure S11) particularly on the STW-influenced northern flank of the rise (Figure S17). The preference for STW influenced waters reported here is consistent with the dominance of prasinophytes assessed from pigment analysis in the STFZ in the SW Pacific (Delizo et al., 2007; DiTullio et al., 2003) and Indian sectors of the Southern Ocean (Iida and Odate, 2014). Broader application of pigment approaches have revealed that prasinophytes can contribute substantially to vernal blooms at temperature latitudes (Bustillos-Guzman et al., 1995; Latasa et al., 2010; Gutiérrez-Rodríguez et al., 2011; Nunes et al., 2018). High abundance of several species of prasinophytes including *Ostreococcus* sp. and *Micromonas* sp. have been recently reported during the onset of the North Atlantic spring bloom from 16S rRNA amplicon sequencing analysis (Bolaños et al., 2020) and at more temperate latitudes of the Eastern North Atlantic using 18S rRNA metabarcoding (Joglar et al., 2021). The deep mixing layers (>100 m) during the New Zealand STW spring bloom II voyage (TAN1212) (Chiswell et al., 2019), where prasinophytes dominated, supports the idea that this picophytoplankton group thrives under high-nutrient, high-mixing conditions playing an important role in the development of spring blooms, characteristic of temperate latitudes. Overall, our results highlight the wide ecological breadth of *Mamiellophyceae* and certain species like *Ostreococcus* sp., which tend to dominate across a wide range of physico-chemical and trophic conditions but with a marked preference for nutrient-rich coastal and oceanic waters (Tragin and Vaulot, 2018; Lopes dos Santos et al., 2017b).

Chloropicophyceae (previously defined as Prasinophytes clade VII, Lopes dos Santos et al. (2017a)) showed an opposite trend to *Mamiellophyceae*, with the highest relative abundance associated with SAW samples (Figs. 5 and 6). Culture representatives of *Chloropicophyceae* and 18S rRNA sequences have been obtained from tropical and subtropical latitudes of the north and south Pacific (Lopes dos Santos et al., 2017a,b; Tragin and Vaulot, 2018) but to our knowledge this is the first report of their presence and high abundance in subantarctic waters. The majority of *Chloropicophyceae* reads were most closely related to (99.5%, ASV_0086) or identified (100%, ASV_0014) as *Chloroparvula pacifica*, which was the most abundant protist ASV found in SAW (Fig. 8). *Chloropicophyceae* has been suggested as the dominant group of green algae in meso- and oligotrophic oceanic waters in contrast with the preference of *Mamiellophyceae* for more nutrient-rich coastal environments (Lopes dos Santos et al., 2017b; Tragin and Vaulot, 2018; Shi et al., 2009). In this study, *Chloropicophyceae* dominated *Chlorophyta* in SAW which are considered HNLC, suggesting that the preference of *Chloropicophyceae* for meso-/oligotrophic conditions reported for typically macronutrient-limited waters could also encompass iron-limited HNLC conditions. Field experiments have suggested that phytoplankton growth in high-latitude HNLC regions is co-limited by B vitamins and iron micronutrients (Panzeca et al., 2006; Bertrand et al., 2007; Koch et al., 2011). Genome analysis of one species of *Chloropicophyceae* (*Chloropicon primus*) indicates that this group might be able to synthesize thiamine, in contrast to *Mamiellophyceae*, which depends on exogenous vitamin B1 or related precursors supplied by B1-synthesizing marine bacteria or other algae (Lemieux et al., 2019; Paerl et al., 2015). The potentially significant ecological role of B1 and B vitamins, in general, in regulating and shaping the taxonomic composition of phytoplankton communities, is rarely considered and is still not well understood (Sañudo Wilhelmy et al., 2014) but could contribute to explaining the contrasting distribution patterns of *Chloropicophyceae* and *Mamiellophyceae*. Interestingly, the abundance of *Chloropicophyceae* was systematically high on Campbell Plateau (Figure S11, Figure S16, Figure S17), an HNLC region where elevated Chl *a* levels are often observed (Banse and English, 1997; Murphy et al., 2001) likely in response to an increase in iron supply (Gutiérrez-Rodríguez et al., 2020). Whether this regional preference was linked to the bathymetric and hydrographic characteristics of the plateau (Neil et al., 2004; Forcén-Vázquez et al., 2021), the natural iron fertilization hypothesized for the region (Banse and English, 1997; Gutiérrez-Rodríguez et al., 2020) or a combination of these and other aspects cannot be concluded from our study and highlights the need of further studies to better understand the ecological drivers beyond coastal-oceanic trophic gradients underpinning the distribution of this *Chloropicophyceae* species.

4.2.2. Dinophyceae (Dinoflagellates)

The relative abundance of both parasitic Syndiniales and *Dinophyceae* in the euphotic zone tended to be higher in SAW and the STF compared to STW metabarcodes (Fig. 5, Fig. 6). The increase of *Dinophyceae* is consistent with previous microscopy-based observations (Chang and Gall, 1998). Dinophyceae includes photosynthetic, mixotrophic and heterotrophic species. In our study, ASVs affiliated to *Gyrodinium* sp. were identified as the most abundant non-syndiniale dinoflagellates in agreement with a previous study in the Southland Current where DNA barcodes of *Gyrodinium*, *Karlodinium* and *Gymnodinium* species were also reported among the most abundant species (Allen et al., 2020). Many *Gyrodinium* species prey on bacteria and algae (Hansen, 1992; Jeong et al., 2008; Jang et al., 2019). They can constitute an important component of phagotrophic protists biomass in coastal and oceanic environments (Sherr and Sherr, 2007; Jeong et al., 2010) including high latitude waters (Archer et al., 1996; Strom et al., 2001; Olson and Strom, 2002) where they have shown the capability of cropping down iron-stimulated diatom blooms (Saito et al., 2006). The

dominance of *Gyrodinium* spp. in our study suggests *Dinophyceae* were an important component of phagotrophic protists in this region as well. While species of *Gyrodinium* were prevalent across all water masses in our study, their abundance was higher in more productive STF waters (Fig. 8, Figure S9), where higher Chl *a* concentrations was accompanied by increased abundance of diatoms and larger phytoplankton cells, confirming their pivotal importance in pelagic foodwebs as the link between primary producers and metazoan zooplankton (Zeldis and Décima, 2020).

4.2.3. Bacillariophyta (Diatoms)

Diatoms tended to be more abundant in the STF metabarcodes compared to STW and SAW although relatively high contributions (>30%) were at times observed in all water masses (Fig. 6) particularly during spring in STW waters and summer-fall period in SAW (Fig. 7, Figure S17). Most abundant ASVs in STF waters belong to *Mediophyceae* species like *Brockmaniella brockmanii*, which has been observed during the onset of the Spring bloom in coastal, temperate waters (Grattepanche et al., 2011) and *Fragilariopsis sublineata/kerguelensis* (Fig. 8, Figure S9). The dominance of the later was mainly due to their abundance in the southern STF flowing north of Campbell Plateau (Figure S11). Several diatom species including *F. sublineata/kerguelensis*, *F. cylindrus*, *Chaetocerus peruvianus*, and *Cylindrotheca closterium* were significantly more abundant in the STF compared to STW, but not compared to SAW (Figure S12) supporting the greater resemblance of diatom assemblages between STF and SAW.

ASVs identified as or most closely related to *F. sublineata/kerguelensis* were in fact the most abundant diatom found in SAW (Fig. 8) in agreement with the preference of *Fragiolariopsis* spp. for SAW as inferred from microscopy (Chang and Gall, 1998). *F. sublineata* has been reported to dominate in sea ice algal biomass and for being well adapted to low light conditions (McMinn et al., 2010). This species is seldom reported in high abundance in oceanic Southern Ocean waters, where other species like *F. curta* and *F. kerguelensis* tend to dominate diatom assemblages (Quéguiner et al., 1997; Olguín and Alder, 2011; Mohan et al., 2011; Gall et al., 2001). While these observations support the identification of *F. sublineata/F. kerguelensis* ASVs as *F. kerguelensis* in our study, these ASVs (e.g., ASV_0036, ASV_0061) had several mismatches and only 99.3% similarity with the partial V4 sequence of both species (Figure S18) suggesting they may belong to different *Fragilariopsis* species. The low silicate characteristics of SAW east of New Zealand (Dugdale et al., 1996) is likely a key factor responsible for the southward (e.g. from Bio-SAM to SAF) increase of heavily silicified diatoms like *Fragilariopsis* spp. (Figure S11) in a way consistent with the tendency of this genus to dominate south of the SAF (Assmy et al., 2013; Pinkernell and Beszteri, 2014). Furthermore, the shift in the relative abundance of the dominant ASVs assigned to *F. sublineata/kerguelensis* (ASV_0036 and ASV_0061) observed between subantarctic waters north (i.e., Bio-SAM, Campbell Plateau) and south of the SAF (Figure S12, Figure S18) suggests potential differences in their silicate requirements. In STW, other small species such as *Minidiscus trioculatus* and *Minutocellus polymorphus* were identified among the most abundant diatoms (Fig. 8, Figure S9), consistent with the dominance of these small diatom taxa in neritic-modified STW of the upstream Southland Current (Allen et al., 2020). While most common genera reported in STW (and STF) by microscopy analysis (e.g. *Thalassiosira* spp., *Chaetoceros* spp., *Guinardia* spp.) were also detected by DNA metabarcoding, the small nano-sized species revealed as numerically dominant by DNA approaches can be overlooked by microscopy (Chang and Gall, 1998). Diatoms are generally conceptualized as the microplankton group associated with new production and high export potential (Legendre and Lefevre, 1995; Vidussi et al., 2001; Uitz et al., 2006). However, there are increasing evidence supporting the importance of small nano- and even pico-sized diatoms in both coastal and oceanic systems (Arsenieff et al., 2020; Buck et al., 2008; Lomas et al., 2009; Hernández-Ruiz et al., 2018). Our results showing the dominance of *M. trioculatus* and *M. polymorphus* in STW, particularly in association with more productive conditions surveyed during the onset of the spring bloom (e.g. TAN1212) and productive conditions of the STF over the Chatham Rise (Figure S10, Figure S11) further support the important role played by small diatoms in driving open-ocean phytoplankton production (Leblanc et al., 2018). Downward fluxes in SAW- and STW-influenced waters on the flanks of the central Chatham Rise during the spring bloom are however dominated by *Chaetoceros* resting spores and *Pseudo-nitzschia* sp. (Wilks et al., 2021), suggesting that the relative contribution of small Polar-centric diatoms such as *M. trioculatus* and *M. polymorphus* to vertical export might be relatively lower compared to their contribution to primary production.

4.2.4. Pelagophyceae

Pelagophyceae showed their lowest abundance in the STF zone (Fig. 6) with increases their relative contribution increased towards SAW (Fig. 5, Fig. 6) in agreement with the dominance of *Pelagophyceae* in nearby SA waters assessed by pigment analysis (DiTullio et al., 2003). The relative abundance of this class and *Pelagomonas* species also decreased following natural or experimental iron addition experiments in HNLC waters of the Southern Ocean (Irion et al., 2020; Thiele et al., 2014). These observations are consistent with the physiological advantage in iron uptake of pelagophytes over other small eukaryotic phytoplankton groups (Timmermans et al., 2005) and indicates a competitive advantage for pelagophytes in oligotrophic ecosystems. Vertically, the relative contribution of this class increased with depth (Fig. 7, Figure S17) in agreement with their preference for deeper layers (Latasa et al., 2017; Cabello et al., 2016; Gall et al., 2008) and their physiological adaptation to low light and relatively higher nutrient conditions characteristic of the subsurface chlorophyll maximum where they often peak in abundance (Dimier et al., 2009; Dupont et al., 2015; Latasa et al., 2022). This vertical segregation was evident in both STW and SAW samples despite differences in species composition between water masses (Fig. 8) (Figure S9). For example, *P. calceolata* is a widespread picoplankton species (Andersen et al., 1996; Moon-van der Staay et al., 2001). Whether the ubiquity of this species is bound to high genetic diversity or physiological versatility is not clear. In our study, several ASVs were assigned to *P. calceolata* (100% similarity) and while the most abundant ASV_0044 showed preference for STW, other less abundant ASVs (e.g. ASV_0625) were significantly more abundant in SAW (Figure S12) supporting the ecological significance of genotypic diversity. Similarly, we found different water mass preferences among unidentified pelagophyte ASVs most closely related to (99.3–99.9%) *A. anophagefferens*, with some preferentially associated with STW or SAW but interestingly none with STF (Figure S12). While these observations suggest that different ASVs may reflect ecologically relevant different units (Rodríguez et al., 2005), it is unclear whether these diversity reflects species or intra-specific variability. These taxonomic gaps highlight the importance of culture isolates and morpho-molecular characterization to better determine the diversity of pelagophytes and its ecological implications.

4.2.5. Prymnesiophyceae

Prymnesiophyceae metabarcodes were prevalent across all water masses (Fig. 5) but tended to be more abundant in SAW (Fig. 6). Overall, their relative contribution to eukaryotic phytoplankton was lower than depicted by pigment-based analyses of open ocean microbial communities (Andersen et al., 1996). The prevalence of 19'hexanoyloxyfucoxanthin pigment marker in oceanic waters and the application of quantitative methods (e.g. CHEMTAX) have shown that *Prymnesiophyceae* represents between 20%–50% of the phytoplankton community in oceanic waters (Andersen et al., 1996; DiTullio et al., 2003; Latasa et al., 2005; Liu et al., 2009; Swan et al., 2016). Such dominance has been also depicted by improved genomic approaches that

revealed the extremely high genetic and functional diversity of non-calcifying prymnesiophytes (Liu et al., 2009; Cuvelier et al., 2010). In our study, non-calcifying species, mainly assigned to *Phaeocystis* spp. and *Chrysochromulina* spp., dominated the group (Figure S9) in agreement with DNA-based studies in the SW Pacific region (Sow et al., 2020; Wolf et al., 2014). The dominance of *Phaeocystis* spp. in SAW was mainly driven by *P. antarctica* (Fig. 8), corresponding with the prominence of this group in the Southern Ocean (Verity et al., 2007) and decreasing abundance observed from SAW towards STW of the SW Pacific region during austral autumn–winter (Sow et al., 2020). These results contrast with the similar spatial distribution *P. antarctica* spp. metabarcodes observed between contrasting conditions on and off the Kerguelen Plateau (Irion et al., 2020). ASVs identical to isolates of *P. globosa* (e.g. ASV_0065, 100%) and *P. cordata* (ASV_0227, 100%) were also detected in all water masses, but unlike *P. antarctica* they tended to be more prevalent and abundant in STW compared to SAW (Sow et al., 2020). Coccolithophores are an important component of phytoplankton communities in the Southern Ocean region extending from the STF to the Polar Front known as the Great Calcite Belt (Chang and Northcote, 2016; Balch et al., 2016; Wilks et al., 2021). ASV_0053 was the most abundant coccolithophore species in our study, particularly in the STF (Figure S9; Figure S11) in agreement with previous microscopy-based studies in this region of the SW Pacific (Saavedra-Pellitero et al., 2014; Chang and Northcote, 2016; Rigual-Hernández et al., 2020) and in the Southern Ocean (Holligan et al., 2010; Balch et al., 2016). The isolation work we conducted with samples collected from SAW and SAF during TAN1702 resulted in 12 cultures identified as *Emiliania huxleyii*, supporting the importance of this species in the region (Chang and Northcote, 2016) while highlighting the limitations of partial sequencing commonly used in DNA metabarcoding approaches to distinguish closely related coccolithophore species.

4.2.6. Cryptophyceae

In our dataset, the contribution of *Cryptophyceae* metabarcodes was relatively low on average (<1%) but showed increasing abundance from SAW to STW (Fig. 6). Similar water-mass preference was depicted by quantitative pigment analysis in the same STFZ region over the Chatham Rise, where cryptophytes contribution in STW (47%–63% chl *a*) was higher than in SAW (6% chl *a*) (Delizo et al., 2007). *Cryptophyta* are an ubiquitous phytoplankton group with widespread distributions from coastal to open oceanic systems and from tropical to polar latitudes (Buma et al., 1992; Piwosz et al., 2013; Nunes et al., 2019). They have been reported to form blooms in coastal embayments (Jeong et al., 2013; Johnson et al., 2013) and Antarctic coastal waters favoured by low salinity conditions (Moline et al., 2004; Nunes et al., 2019; Schofield et al., 2017). The higher contributions we observed in STW relative to SAW, however, argue against the direct influence of salinity on cryptophytes at least in open-ocean waters. These low salinity conditions are typically produced by ice melting which promotes the stratification the upper water column and releases iron that stimulates phytoplankton growth (Lannuzel et al., 2016). Cryptophytes have been also observed to respond positively to iron fertilization in HNLC waters of the North Pacific (Sato et al., 2009; Suzuki et al., 2009) suggesting that their low abundance in SAW in our study and high abundance in low salinity Antarctic waters (Moline et al., 2004; Nunes et al., 2019; Schofield et al., 2017) could be related to differences in iron-limited conditions between both regions. The contribution of cryptophytes in STW was highest during the open-ocean spring bloom (Spring Bloom II-TAN1212 voyage) and in shelf-slope stations of the EAUC current (Cross-shelf Exchange-TAN1604 voyage) consistent with their preference for more nutrient-rich conditions (Fuller et al., 2006; Latasa et al., 2010; Carreto et al., 2016). Significant contributions by cryptophytes has also been observed in open ocean waters of the NW Mediterranean at the termination of the spring bloom (Vidussi et al., 2000) where they even dominated the surface mixed layer community at highly stratified stations. Interestingly, the higher contribution of cryptophytes in our study occurred towards the end of the spring bloom (TAN1212) (Figure S17), coincident with strong surface stratification and biomass accumulation (Chiswell et al., 2019), and supporting the importance that stratification may have on this group compared to salinity. *Geminigera cryophile* and other species of *Teleaulax* have been reported as mixotrophic (Schneider et al., 2020), which could favour their increase in later stages of the spring bloom when the coincident decrease of nutrients and increase of potential prey tend to favour mixotrophy (Mitra et al., 2014).

4.3. Heterotrophic and mixotrophic protists below the euphotic zone

We used the samples collected during six voyages of the Biophysical Moorings time-series between 2009–2012 to investigate the protistan community composition below the euphotic zone (Table 1). Here, Syndiniales dominated the metabarcode dataset in agreement with other metabarcoding surveys that have reported the dominance of this group of parasites (Guillou et al., 2008; Vargas et al., 2015; Giner et al., 2020). Radiolaria, a common host of Syndiniales (Bråte et al., 2012), became the most abundant group after removing sequences assigned to Syndiniales (Fig. 7). Radiolaria, a holoplanktonic amoeboid group with widespread distribution in modern oceans (Suzuki and Not, 2015; Biard et al., 2016), are mainly heterotrophic protists with many mixotrophic species in the photic zone bearing endosymbiotic microalgae (Caron et al., 1995; Decelle et al., 2015). While Radiolaria are found throughout the entire water column, their contribution to plankton biomass (Biard et al., 2016; Boltovskoy and Correa, 2016) and metabarcodes (Giner et al., 2020; Ollison et al., 2021) tends to be greater in the mesopelagic ocean, in a way consistent with our metabarcoding results. In the present study, significant contributions of Radiolaria were mainly constrained to the aphotic zone (Fig. 7). This depth-related pattern, contrasts with previously reported abundance of Radiolaria, and symbiotic Collodaria, in the sunlit ocean (Vargas et al., 2015). We found substantial contributions of photosymbiotic Collodaria at times, particularly in SAW (Figure S9), but the vertical distribution of Radiolaria below the euphotic zone suggested they were mainly composed of heterotrophic species. The high copy number of 18S rDNA in Radiolaria may contribute to their high relative abundance in metabarcode datasets (Vargas et al., 2015; Gutierrez-Rodriguez et al., 2019); however, it is unlikely to be responsible for their dominance, particularly in relation to dinoflagellates and ciliates, which are known to also have high copy numbers (Gong et al., 2013; Piredda et al., 2017). Moreover, the positive relationship between cell length and 18S rDNA copy number (Zhu et al., 2005; Biard et al., 2017) and the higher C and *N* density (mass: volume) of Radiolaria compared to other protists (Mansour et al., 2021) suggest that gene-based relative abundance of these groups was likely reflected in their relative contribution to the total community biomass.

Utilizing their sticky pseudopodia and large size, Radiolaria dwelling below the euphotic zone can effectively intercept sinking particles and act as flux-feeders influencing the quality and quantity of vertical fluxes (Ohman et al., 2012; Stukel et al., 2019). The presence of mineral skeletons, made of silica (Polycystinean groups) or strontium sulfate (e.g. Acantharea), provides substantial mineral ballast (Takahashi, 1983) conferring them a key role in vertical export that is supported by their common presence in sediment traps (Bernstein et al., 1987; Michaels et al., 1995; Gutierrez-Rodriguez et al., 2019; Preston et al., 2020; Prebble et al., 2013) and their enrichment in suspended and sinking particles (Duret et al., 2020). Despite their abundance and their important role in biogeochemical processes (Biard et al., 2016; Guidi et al., 2016) little is known about the vertical distribution of Radiolaria particularly in the meso- and bathypelagic ocean (>500 m) (Boltovskoy, 2017; Biard and Ohman, 2020; Ollison et al., 2021; Llopis Monferrer et al., 2021). In our study, we found an opposite distribution between Acantharea and RAD-B, which showed preference for the upper (<500 m) and deeper (>500 m) mesopelagic samples, respectively

(Fig. 7). Among Acantharea, most sequences were assigned to the order *Chaunchantida* (Figure S9, Figure S15), which has been found in sinking particles collected in the Southern Ocean (Duret et al., 2020) and the California Current (Gutierrez-Rodriguez et al., 2019; Preston et al., 2020). In a recent study conducted in the Southern Ocean, RAD B was reported to be enriched in small (<10 μm) suspended particles relative to sinking particles (Duret et al., 2020) while RAD-A were consistently found in sinking particles reaching abyssal depths in the California Current Ecosystem (Preston et al., 2020). The higher contribution of RAD-B relative to RAD-A we found in our study is consistent with the tendency of RAD-B to remain suspended compared to RAD-A, which had greater sinking potential. Among the polycystinean Radiolaria, Spumellaria was the most important order, in a way consistent with observed abundance of this order in sinking particulate organic matter collected in sediment traps deployed in mesopelagic and abyssal depths in the California Current Ecosystem (Gutierrez-Rodriguez et al., 2019; Preston et al., 2020). Several ASVs assigned to Spumellaria Group I were among the most abundant species in our study (Figure S14). Interestingly, some of these ASVs showed preference for SAW while others were more abundant in STW, highlighting the need to improve our taxonomic knowledge of this group.

Relative contributions of ciliates were also higher below the euphotic zone, mainly driven by ASVs affiliated with the *Spirotrichea* class (Grattepanche et al., 2016). Most abundant ASVs assigned to the order Strombidiida (Oligotrichia, Spirotrichea) and *Leegaardiella* sp. (Choreotrichia, Spirotrichea), which have been reported below the euphotic zone at meso- and bathy-pelagic depths (Grattepanche et al., 2016; Duret et al., 2020). In addition to Spirotrichea, class Oligohymenophorea and Nassophorea contributed substantially in both STW and SAW, mainly sustained by ASVs assigned to OLIGO5 (*Oligophymenophorea*) and *Discotrichidae* (*Nassophorea*), both previously reported in mesopelagic waters (Duret et al., 2020). The dominance of these groups was consistent across different water masses off eastern New Zealand although some species like *Leegaardiella* (Oligotrichia) and *Strombidium_k_*sp (Choreotrichia) showed preference for STW and SAW, respectively (Figure S12). Ciliates below the euphotic zone feed on bacteria and small protists associated with particulate organic matter (Caron et al., 2012). Several species also have the potential to engage in photoautotrophy and phagotrophy (Leles et al., 2017). By doing so, ciliates play an important role within planktonic food webs contributing to trophic transfer and nutrient recycling in the dark ocean. The high taxonomic diversity and abundance of heterotrophic protists in this and previous studies (Zoccarato et al., 2016; Grattepanche et al., 2016; Duret et al., 2020; Ollison et al., 2021) highlights their importance in planktonic systems below the euphotic zone and emphasizes how little we know about their ecological role in the food web functioning. Further studies focusing on the taxonomic and functional diversity of heterotrophic protists have the potential to shed light on the trophic and biogeochemical processes that transform organic matter in the dark ocean, and hence significantly improve our understanding of the biological carbon pump and natural deep-ocean carbon sequestration.

5. Conclusions

The spatial diversity patterns observed in the New Zealand sector of the SW Pacific Ocean are in agreement with global trends of decreasing diversity at higher latitudes and in colder waters. However, deviations from this general pattern were also observed regionally. Species richness and diversity of protist communities in the STF were systematically lower compared to adjacent STW and SAW waters in the northern and southern regions of the STFZ, highlighting the importance of physical oceanographic features in determining regional diversity. Increasing diversity from spring through to summer and autumn observed in both STW and SAW suggested similar influences of seasonal variability across water masses. Dinoflagellates and green algae co-dominated the protistan community in the euphotic zone but water-mass specificity emerging at lower taxonomic levels within these and other major taxonomic groups. Despite different seasons and regions that were included in our study, protistan community composition varied consistently between water masses. Within green algae for instance, *Mamiellophyceae* dominated in STW driven by several species showing different regional abundances, while *Chloropicophyceae* became dominant in SAW where several ASVs assigned to *Chloroparvula pacifica* appeared among the most abundant taxa. Interestingly, other less abundant ASVs identified as *Chloroparvula pacifica* showed statistically significant preferences for STW. Analogous strain specific variability was observed for ASVs assigned to species belonging to other phytoplankton classes with widespread distribution (e.g. *P. antarctica*, prymnesiophytes; *P. calceolata*, pelagophytes) suggesting the genotypic diversity may be linked to ecological traits that influence distribution patterns of phytoplankton. Although Chl *a* levels comprised in this study were relatively low, the dominance of pico- and nano-Chl *a* fractions together with the numerical dominance of small taxa (e.g. Mamiellophyceae) revealed by DNA metabarcoding, indicates that small rather than large taxa dominate the phytoplankton community during spring bloom conditions and in the highly STFZ suggesting that picoplankton can also escape grazing control and drive phytoplankton proliferations under favourable conditions. The mesopelagic zone was clearly dominated by radiolarian sequences, supporting the importance of this group for the functioning of the dark ocean. Taxonomic assignation revealed a diverse assemblage of Radiolaria and a taxon-specific water mass and vertical distribution patterns. However, further research is needed about the ecology of these organisms to link this compositional diversity to their functioning in the mesopelagic system.

CRediT authorship contribution statement

Andres Gutiérrez-Rodríguez: Conceptualization, Methodology, Formal analysis, Investigation, Data curation, Visualization, Writing – original draft, Funding acquisition. **Adriana Lopes dos Santos:** Conceptualization, Methodology, Investigation, Data curation, Writing – original draft, Funding acquisition. **Karl Safi:** Investigation, Writing – review & editing. **Ian Probert:** Conceptualization, Writing – review & editing, Funding acquisition. **Fabrice Not:** Conceptualization, Writing – review & editing, Funding acquisition. **Denise Fernández:** Conceptualization, Writing – review & editing. **Priscillia Gourvil:** Methodology, Investigation and data curation, Review & editing. **Jaret Bilewitch:** Methodology, Writing – review & editing. **Debbie Hulston:** Methodology, Writing – review & editing. **Matt Pinkerton:** Writing – review & editing, Funding acquisition. **Scott D. Nodder:** Conceptualization, Investigation, Data curation, Writing – original draft, Writing – review & editing, Funding acquisition.

Declaration of competing interest

The authors declare that they have no known competing financial interests or personal relationships that could have appeared to influence the work reported in this paper.

Acknowledgements

We acknowledge the crew and scientific complements of RV *Tangaroa* and RV *Kaharoa* for their efforts in facilitating the sampling throughout all the voyages included in this work. We thank Els Maas and Cliff Law for collecting DNA samples during KAH1303 voyage and for sharing the physical and chemical data obtained on this voyage. Thank you to Daniel Vaulot for critical feedback on PR2 references and assignation. We are thankful to the anonymous reviewers for their efforts and constructive comments that helped improve the manuscript. We are grateful to the Royal Society of New Zealand which funded this research through the Catalyst Seeding General fund (grant reference

number 16-NIW-009-CSG) and fostered the collaboration between the Station Biologique de Roscoff and NIWA. This work is also supported by NIWA via the New Zealand Ministry of Business, Innovation and Employment's Strategic Science Investment Funding to the National Coasts and Oceans Centre. ALS was supported by the Singapore Ministry of Education, Academic Research Fund Tier 1 (RG26/19).

Appendix A. Supplementary data

Supplementary material related to this article can be found online at https://doi.org/10.1016/j.pocean.2022.102809.

References

Agogué, H., Lamy, D., Neal, P., Sogin, M.L., Herndl, G.J., 2011. Water mass-specificity of bacterial communities in the North Atlantic revealed by massively parallel sequencing. Mol. Ecol. 20 (2), 258–274, Publisher: John Wiley & Sons, Ltd.

Allen, R., Summerfield, T., Currie, K., Dillingham, P., 2020. Distinct processes structure bacterioplankton and protist communities across an oceanic front. Aquat. Microb. Ecol. 85, 19–34.

Andersen, R.A., Bidigare, R.R., Keller, M.D., Latasat, M., 1996. A comparison of HPLC pigment signatures and electron microscopic observations for oligotrophic waters of the north atlantic and Pacific oceans. Oceans 43 (2), 517–537.

Archer, S.D., Leakey, R.J.G., Burkill, P.H., Sleigh, M.A., 1996. Microbial dynamics in coastal waters of east antarctica: herbivory by heterotrophic dinoflagellates. Mar. Ecol. Prog. Ser. 139 (1), 239–255, Publisher: Inter-Research Science Center.

Arsenieff, L., Le Gall, F., Rigaut-Jalabert, F., Mahé, F., Sarno, D., Gouhier, L., Baudoux, A.-C., Simon, N., 2020. Diversity and dynamics of relevant nanoplanktonic diatoms in the western english channel. ISME J. 14, 1966–1981.

Assmy, P., Smetacek, V., Montresor, M., Klaas, C., Henjes, J., Strass, V.H., Arrieta, J.M., Bathmann, U., Berg, G.M., Breitbarth, E., Cisewski, B., Friedrichs, L., Fuchs, N., Herndl, G.J., Jansen, S., Krägefsky, S., Latasa, M., Peeken, I., Röttgers, R., Scharek, R., Schüller, S.E., Steigenberger, S., Webb, A., Wolf-Gladrow, D., 2013. Thick-shelled, grazer-protected diatoms decouple ocean carbon and silicon cycles in the iron-limited Antarctic Circumpolar Current. Proc. Natl. Acad. Sci. USA 110 (51), 20633–20638.

Baird, R.B., 2017. Standard methods for the examination of water and wastewater, 23rd. Publisher: Water Environment Federation, American Public Health Association, American.

Balch, W.M., Bates, N.R., Lam, P.J., Twining, B.S., Rosengard, S.Z., Bowler, B.C., Drapeau, D.T., Garley, R., Lubelczyk, L.C., Mitchell, C., Rauschenberg, S., 2016. Factors regulating the great calcite belt in the southern ocean and its biogeochemical significance. Glob. Biogeochem. Cycles 30 (8), 1124–1144, Publisher: Blackwell Publishing Ltd.

Baltar, F., Currie, K., Stuck, E., Roosa, S., Morales, S.E., 2016. Oceanic fronts: transition zones for bacterioplankton community composition. Environ. Microbiol. Rep. 8 (1), 132–138, ISBN: 1758-2229 (Electronic) 1758-2229 (Linking).

Banse, K., 1996. Low seasonality of low concentrations of surface chlorophyll in the subantarctic water ring: Underwater irradiance, iron, or grazing? Prog. Oceanogr. 37 (3), 241–291, Publisher: Elsevier Ltd.

Banse, K., English, D.C., 1997. Near-surface phytoplankton pigment from the coastal zone color scanner in the subantarctic region southeast of New Zealand. Mar. Ecol. Prog. Ser. 156, 51–66, ISBN: 0171-8630.

Barnett, D.J., Arts, I.C., Penders, J., 2021. microViz: an R package for microbiome data visualization and statistics. J. Open Source Softw. 6 (63), 3201.

Barton, A.D., Dutkiewicz, S., Flierl, G., Bragg, J., Follows, M.J., 2010. Patterns of diversity in marine phytoplankton. Science 327 (5972), 1509 LP – 1511, URL http://science.sciencemag.org/content/327/5972/1509.abstract.

Behrens, E., Hogg, A.M., England, M.H., Bostock, H., 2021. Seasonal and interannual variability of the subtropical front in the New Zealand region. J. Geophys. Res. Oceans 126 (2), e2020JC016412 Publisher: Wiley Online Library.

Belkin, I.M., Gordon, A.L., 1996. Southern Ocean fronts from the Greenwich meridian to Tasmania. J. Geophys. Res. Oceans 101, 3675–3696, Publisher: Wiley Online Library.

Bernstein, R.E., Betzer, P.R., Feely, R.A., Byrne, R.H., Lamb, M.F., Michaels, A.F., 1987. Acantharian fluxes and strontium to chlorinity ratios in the north Pacific ocean. Science 237 (4821), 1490–1494, ISBN: 0036-8075.

Bertrand, E.M., Saito, M.A., Rose, J.M., Riesselman, C.R., Lohan, M.C., Noble, A.E., Lee, P.A., DiTullio, G.R., 2007. Vitamin B12 and iron colimitation of phytoplankton growth in the ross sea. Limnol. Oceanogr. 52 (3), 1079–1093, Publisher: Wiley Online Library.

Biard, T., Bigeard, E., Audic, S., Poulain, J., Gutierrez-Rodriguez, A., Pesant, S., Stemmann, L., Not, F., 2017. Biogeography and diversity of Collodaria (Radiolaria) in the global ocean. Isme J. 11 (6), 1331–1344, ISBN: 1751-7362.

Biard, T., Ohman, M.D., 2020. Vertical niche definition of test-bearing protists (Rhizaria) into the twilight zone revealed by in situ imaging. Limnol. oceanogr..

Biard, T., Stemmann, L., Picheral, M., Mayot, N., Vandromme, P., Hauss, H., Gorsky, G., Guidi, L., Kiko, R., Not, F., 2016. In situ imaging reveals the biomass of giant protists in the global ocean. Nature 532 (7600), 504–507, ISBN: 1476-4687 (Electronic) 0028-0836 (Linking).

Bolaños, L.M., Karp-Boss, L., Choi, C.J., Worden, A.Z., Graff, J.R., Haëntjens, N., Chase, A.P., Della Penna, A., Gaube, P., Morison, F., Menden-Deuer, S., Westberry, T.K., O'Malley, R.T., Boss, E., Behrenfeld, M.J., Giovannoni, S.J., 2020. Small phytoplankton dominate western North Atlantic biomass. ISME J. 1–12, Publisher: Springer US.

Boltovskoy, D., 2017. Vertical distribution patterns of Radiolaria Polycystina (Protista) in the world ocean: living ranges, isothermal submersion and settling shells. J. Plankton Res. 39 (2), 330–349, ISBN: 0142-7873.

Boltovskoy, D., Correa, N., 2016. Biogeography of radiolaria polycystina (protista) in the world ocean. Prog. Oceanogr. 149, 82–105, ISBN: 0079-6611.

Bowen, M., Sutton, P., Roemmich, D., 2014. Estimating mean dynamic topography in boundary currents and the use of a rgo trajectories. J. Geophys. Res. Oceans 119 (12), 8422–8437, Publisher: Wiley Online Library.

Boyd, P., Claustre, H., Levy, M., Siegel, D.A., Weber, T., 2019. Multi-faceted particle pumps drive carbon sequestration in the ocean. Nature 568 (7752), 327–335, URL http://www.nature.com/articles/s41586-019-1098-2.

Boyd, P., LaRoche, J., Gall, M., Frew, R., McKay, R.M.L., 1999. Role of iron, light, and silicate in controlling algal biomass in subantarctic waters SE of New Zealand. J. Geophys. Res. Oceans 104, 13395–13408, Publisher: American Geophysical Union (AGU).

Boyd, P.W., Strzepek, R., Fu, F., Hutchins, D.A., 2010. Environmental control of open-ocean phytoplankton groups: Now and in the future. Limnol. Oceanogr. 55 (3), 1353–1376.

Bradford-Grieve, J.M., Boyd, P.W., Chang, F.H., Chiswell, S., Hadfield, M., Hall, J.A., James, M.R., Nodder, S.D., Shushkina, E.A., 1999. Pelagic ecosystem structure and functioning in the Subtropical front region east of New Zealand in austral winter and spring 1993. J. Plankton Res. 21 (3), 405–428.

Bradford-Grieve, J.M., Chang, F.H., Gall, M., Pickmere, S., Richards, F., 1997. Size-fractionated phytoplankton standing stocks and primary production during austral winter and spring 1993 in the Subtropical Convergence region near New Zealand. New Zealand J. Mar. Freshw. Res. 31 (2), 201–224, ISBN: 0028-8330 1175-8805.

Bråte, J., Krabberød, A.K., Dolven, J.K., Ose, R.F., Kristensen, T., Bjørklund, K.R., Shalchian-Tabrizi, K., 2012. Radiolaria associated with large diversity of marine alveolates. Protist 163 (5), 767–777, URL https://www.sciencedirect.com/science/article/pii/S1434461012000387.

Buck, K.R., Chavez, F.R., Davis, A.S., 2008. Minidiscus trioculatus, a small diatom with a large presence in the upwelling systems of central California. Nova Hedwigia 1–6, Publisher: GEBRUDER BORNTRAEGER JOHANNESSTR 3A, D-70176 STUTTGART, GERMANY.

Buma, A.G.J., Gieskes, W.W.C., Thomsen, H.A., 1992. Abundance of cryptophyceae and chlorophyll b-containing organisms in the weddell-scotia confluence area in the spring of 1988. In: Weddell Sea Ecology. Springer, pp. 43–52.

Bustillos-Guzman, J., Claustre, H., Marty, J.-c., 1995. Specific phytoplankton signatures and their relationship to hydrographic conditions in the coastal northwestern mediterranean sea. Mar. Ecol. Prog. Ser. 124, 247–258.

Cabello, A.M., Latasa, M., Forn, I., Morán, X.A.G., Massana, R., 2016. Vertical distribution of major photosynthetic picoeukaryotic groups in stratified marine waters. Environ. Microbiol. 18 (5), 1578–1590, Publisher: Wiley Online Library.

Calbet, A., Landry, M., 2004. Phytoplankton growth, microzooplankton grazing, and carbon cycling in marine systems. Limnol. Oceanogr. 49 (1), 51–57.

Calbet, a., Saiz, E., 2005. The ciliate-copepod link in marine ecosystems. Aquat. Microb. Ecol. 38, 157–167.

Callahan, B.J., McMurdie, P.J., Holmes, S.P., 2017. Exact sequence variants should replace operational taxonomic units in marker-gene data analysis. ISME J. 11 (12), 2639–2643, Publisher: Nature Publishing Group.

Caron, D.A., Countway, P.D., Jones, A.C., Kim, D.Y., Schnetzer, A., 2012. Marine protistan diversity. Ann. Rev. Mar. Sci. 4 (1), 467–493, Publisher: Annual Reviews.

Caron, D.A., Michaels, A.F., Swanberg, N.R., Howse, F.A., 1995. Primary productivity by symbiont-bearing sarcodine (Acantharia, Radiolaria, Foraminifera) in surface waters near Bermuda. J. Plankton Res. 17 (1), 103–129, ISBN: 0142-7873.

Carreto, J.I., Montoya, N.G., Carignan, M.O., Akselman, R., Acha, E.M., Derisio, C., 2016. Environmental and biological factors controlling the spring phytoplankton bloom at the Patagonian shelf-break front - Degraded fucoxanthin pigments and the importance of microzooplankton grazing. Prog. Oceanogr. 146, 1–21, Publisher: Elsevier Ltd.

Cavicchioli, R., Ripple, W.J., Timmis, K.N., Azam, F., Bakken, L.R., Baylis, M., Behrenfeld, M.J., Boetius, A., Boyd, P.W., Classen, A.T., Crowther, T.W., Danovaro, R., Foreman, C.M., Huisman, J., Hutchins, D.A., Jansson, J.K., Karl, D.M., Koskella, B., Mark Welch, D.B., Martiny, J.B.H., Moran, M.A., Orphan, V.J., Reay, D.S., Remais, J.V., Rich, V.I., Singh, B.K., Stein, L.Y., Stewart, F.J., Sullivan, M.B., van Oppen, M.J.H., Weaver, S.C., Webb, E.A., Webster, N.S., 2019. Scientists' warning to humanity: microorganisms and climate change. Nat. Rev. Microb. 17 (9), 569–586.

Chang, F.H., Gall, M., 1998. Phytoplankton assemblages and photosynthetic pigments during winter and spring in the subtropical convergence region near New Zealand. New Zealand J. Mar. Freshw. Res. 32 (4), 515–530, ISBN: 0028-8330 1175-8805.

Chang, F.H., Northcote, L., 2016. Species composition of extant coccolithophores including twenty six new records from the southwest Pacific near New Zealand. Mar. Biodivers. Rec. 9 (1), ISBN: 1755-2672.

Chang, F.H., Zeldis, J., Gall, M., Hall, J., 2003. Seasonal and spatial variation of phytoplankton assemblages, biomass and cell size from spring to summer across the north-eastern New Zealand continental shelf. J. Plankton Res. 25 (7), 737–758, ISBN: 0142-7873.

Chiswell, S.M., 2001. Eddy energetics in the subtropical front over the chatham rise, new zealand. New Zealand J. Mar. Freshw. Res. 35 (1), 1–15, Publisher: Taylor & Francis.

Chiswell, S.M., 2013. Circulation within the Wairarapa Eddy, New Zealand. New Zealand J. Mar. Freshw. Res. 37 (4), 691–704, Publisher: Taylor & Francis.

Chiswell, S.M., Bostock, H.C., Sutton, P.J.H., Williams, M.J.M., 2015. Physical oceanography of the deep seas around New Zealand: a review. New Zealand J. Mar. Freshw. Res. 49 (2), 286–317, ISBN: 0028-8330 1175-8805.

Chiswell, S.M., Safi, K.A., Sander, S.G., Strzepek, R., Ellwood, M.J., Milne, A., Boyd, P.W., 2019. Exploring mechanisms for spring bloom evolution: contrasting 2008 and 2012 blooms in the southwest Pacific ocean. J. Plankton Res. 41 (3), 329–348.

Cuvelier, M.L., Allen, A.E., Monier, A., McCrow, J.P., Messié, M., Tringe, S.G., Woyke, T., Welsh, R.M., Ishoey, T., Lee, J.-H., Binder, B.J., DuPont, C.L., Latasa, M., Guigand, C., Buck, K.R., Hilton, J., Thiagarajan, M., Caler, E., Read, B., Lasken, R.S., Chavez, F.P., Worden, A.Z., 2010. Targeted metagenomics and ecology of globally important uncultured eukaryotic phytoplankton. Proc. Natl. Acad. Sci. USA 107 (33), 14679–14684.

Deacon, G., 1982. Physical and biological zonation in the Southern Ocean. Deep Sea Res. A Oceanogr. Res. Pap. 29 (1), 1–15.

Decelle, J., Colin, S., Foster, R.A., 2015. Photosymbiosis in marine planktonic protists. pp. 465–500. http://dx.doi.org/10.1007/978-4-431-55130-0_19.

Delizo, L., Smith, W.O., Hall, J., 2007. Taxonomic composition and growth rates of phytoplankton assemblages at the subtropical convergence east of New Zealand. J. Plankton Res. 29 (8), 655–670, tex.mendeley-tags: group-specific.

Dimier, C., Brunet, C., Geider, R., Raven, J., 2009. Growth and photoregulation dynamics of the picoeukaryote pelagomonas calceolata in fluctuating light. Limnol. Oceanogr. 54 (3), 823–836, Publisher: Wiley Online Library.

DiTullio, G.R., Geesey, M.E., Jones, D.R., Daly, K.L., Campbell, L., Smith, Jr., W.O., 2003. Phytoplankton assemblage structure and primary productivity along 170 W in the South Pacific Ocean. Mar. Ecol. Prog. Ser. 255, 55–80.

Dugdale, R.C., Wilkerson, F.P., Minas, H.J., 1996. The role of a silicate pump in driving new production. Deep Sea Res. I 42 (5), 697–719.

Dupont, C.L., McCrow, J.P., Valas, R., Moustafa, A., Walworth, N., Goodenough, U., Roth, R., Hogle, S.L., Bai, J., Johnson, Z.I., 2015. Genomes and gene expression across light and productivity gradients in eastern subtropical Pacific microbial communities. ISME J. 9 (5), 1076–1092, Publisher: Nature Publishing Group.

Duret, M.T., Lampitt, R.S., Lam, P., 2020. Eukaryotic influence on the oceanic biological carbon pump in the Scotia sea as revealed by 18S rRNA gene sequencing of suspended and sinking particles. Limnol. Oceanogr. 65 (1), S49–S70.

Ellwood, M.J., Bowie, A.R., Baker, A., Gault-Ringold, M., Hassler, C., Law, C.S., Maher, W.A., Marriner, A., Nodder, S., Sander, S., Stevens, C., Townsend, A., van der Merwe, P., Woodward, E.M.S., Wuttig, K., Boyd, P.W., 2018. Insights into the biogeochemical cycling of iron, nitrate, and phosphate across a 5,300 km south pacific zonal section (153° E–150°W). Glob. Biogeochem. Cycles 32 (2), 187–207, Publisher: Blackwell Publishing Ltd.

Ellwood, M.J., Law, C.S., Hall, J., Woodward, E.M.S., Strzepek, R., Kuparinen, J., Thompson, K., Pickmere, S., Sutton, P., Boyd, P.W., 2013. Relationships between nutrient stocks and inventories and phytoplankton physiological status along an oligotrophic meridional transect in the tasman sea. Deep-Sea Res. I-Oceanogr. Res. Pap. 72, 102–120, ISBN: 0967-0637.

Fernandez, D., Bowen, M., Sutton, P., 2018. Variability, coherence and forcing mechanisms in the New Zealand ocean boundary currents. Prog. Oceanogr. 165, 168–188, Publisher: Elsevier.

Field, C.B., Behrenfeld, M.J., Randerson, J.T., Falkowski, P.G., 1998. Primary production of the biosphere: Integrating terrestrial and oceanic components. Science 281 (5374), 237–240, ISBN: 0036-8075.

Forcén-Vázquez, A., Williams, M.J.M., Bowen, M., Carter, L., Bostock, H., 2021. Frontal dynamics and water mass variability on the Campbell Plateau. New Zealand J. Mar. Freshw. Res. 55 (1), 199–222, Publisher: Taylor & Francis.

Fuhrman, J.A., Steele, J.A., Hewson, I., Schwalbach, M.S., Brown, M.V., Green, J.L., Brown, J.H., 2008. A latitudinal diversity gradient in planktonic marine bacteria. Proc. Natl. Acad. Sci. 105 (22), 7774 LP – 7778.

Fuller, N.J., Tarran, G.a., Cummings, D.G., Woodward, E.M.S., Orcutt, K.M., Yallop, M., Le Gall, F., Scanlan, D.J., 2006. Molecular analysis of photosynthetic picoeukaryote community structure along an Arabian Sea transect. (ISSN: 0024-3590) http://dx.doi.org/10.4319/lo.2006.51.6.2502, ISBN: 0024-3590.

Galand, P.E., Potvin, M., Casamayor, E.O., Lovejoy, C., 2010. Hydrography shapes bacterial biogeography of the deep Arctic Ocean. ISME J. 4 (4), 564–576.

Gall, M., Boyd, P., Hall, J., Safi, K., Chang, H., 2001. Phytoplankton processes. Part 1: community structure during the Southern Ocean iron release experiment (SOIREE). Deep Sea Res. II Top. Stud. Oceanogr. 48 (11), 2551–2570, Publisher: Elsevier.

Gall, F.L., Rigaut-Jalabert, F., Marie, D., Garczarek, L., Viprey, M., Gobet, A., Vaulot, D., 2008. Picoplankton diversity in the south-east pacific ocean from cultures. Biogeosciences 5 (1), 203–214, Publisher: Copernicus GmbH.

Gardner, W.D., Chung, S.P., Richardson, M.J., Walsh, I.D., 1995. The oceanic mixed-layer pump. Deep Sea Res. II Top. Stud. Oceanogr. 42 (2), 757–775, Publisher: Elsevier.

Giner, C.R., Pernice, M.C., Balagué, V., Duarte, C.M., Gasol, J.M., Logares, R., Massana, R., 2020. Marked changes in diversity and relative activity of picoeukaryotes with depth in the world ocean. ISME J. 14 (2), 437–449, Publisher: Nature Publishing Group.

Gong, J., Dong, J., Liu, X., Massana, R., 2013. Extremely high copy numbers and polymorphisms of the rDNA operon estimated from single cell analysis of oligotrich and peritrich ciliates. PROTIST 164 (3), 369–379.

Grattepanche, J.-D., Breton, E., Brylinski, J.-M., Lecuyer, E., Christaki, U., 2011. Succession of primary producers and micrograzers in a coastal ecosystem dominated by phaeocystis globosa blooms. J. Plankton Res. 33 (1), 37–50.

Grattepanche, J.-D., Santoferrara, L.F., McManus, G.B., Katz, L.A., 2016. Unexpected biodiversity of ciliates in marine samples from below the photic zone. Mol. Ecol. 25 (16), 3987–4000, Publisher: John Wiley & Sons, Ltd.

Guidi, L., Chaffron, S., Bittner, L., Eveillard, D., Larhlimi, A., Roux, S., Darzi, Y., Audic, S., Berline, L., Brum, J.R., Coelho, L.P., Espinoza, J.C.I., Malviya, S., Sunagawa, S., Dimier, C., Kandels-Lewis, S., Picheral, M., Poulain, J., Searson, S., Stemmann, L., Not, F., Hingamp, P., Speich, S., Follows, M., Karp-Boss, L., Boss, E., Ogata, H., Pesant, S., Weissenbach, J., Wincker, P., Acinas, S.G., Bork, P., de Vargas, C., Iudicone, D., Sullivan, M.B., Raes, J., Karsenti, E., Bowler, C., Gorsky, G., Tara Oceans Consortium, C., 2016. Plankton networks driving carbon export in the oligotrophic ocean. Nature 532 (7600), 465–+, ISBN: 0028-0836.

Guillou, L., Viprey, M., Chambouvet, A., Welsh, R.M., Kirkham, A.R., Massana, R., Scanlan, D.J., Worden, A.Z., 2008. Widespread occurrence and genetic diversity of marine parasitoids belonging to Syndiniales (Alveolata). Environ. Microbiol. 10 (12), 3349–3365, Publisher: John Wiley & Sons, Ltd.

Gutiérrez-Rodríguez, A., Latasa, M., Scharek, R., Massana, R., Vila, G., Gasol, J.M., 2011. Growth and grazing rate dynamics of major phytoplankton groups in an oligotrophic coastal site. Estuar. Coast. Shelf Sci. 95 (1), 77–87.

Gutiérrez-Rodríguez, A., Safi, K., Fernández, D., Forcén-Vázquez, A., Gourvil, P., Hoffmann, L., Pinkerton, M., Sutton, P., Nodder, S.D., 2020. Decoupling between phytoplankton growth and microzooplankton grazing enhances productivity in subantarctic waters on campbell plateau, southeast of new zealand. J. Geophys. Res. Oceans 125 (2), e2019JC015550 Publisher: John Wiley & Sons, Ltd.

Gutierrez-Rodriguez, A., Stukel, M.R., dos Santos, A., Biard, T., Scharek, R., Vaulot, D., Landry, M.R., Not, F., 2019. High contribution of Rhizaria (Radiolaria) to vertical export in the California Current Ecosystem revealed by DNA metabarcoding. ISME J. 13 (4), 964–976.

Hall, J.A., James, M.R., Bradford-Grieve, J.M., 2001. Structure and dynamics of the pelagic microbial food web of the Subtropical Convergence region east of New Zealand. Aquat. Microb. Ecol. 20 (1), 95–105.

Hall, J.A., Safi, K., James, M.R., Zeldis, J., Weatherhead, M., 2006. Microbial assemblage during the spring-summer transition on the northeast continental shelf of New Zealand. New Zealand J. Mar. Freshw. Res. 40 (1), 195–210.

Hamilton, A.K., Lovejoy, C., Galand, P.E., Ingram, R.G., 2008. Water masses and biogeography of picoeukaryote assemblages in a cold hydrographically complex system. Limnol. Oceanogr. 53 (3), 922–935, Publisher: John Wiley & Sons, Ltd.

Hansen, P.J., 1992. Prey size selection, feeding rates and growth dynamics of heterotrophic dinoflagellates with special emphasis on Gyrodinium spirale. Mar. Biol. 114 (2), 327–334, Publisher: Springer.

Heath, R.A., 1985. A review of the physical oceanography of the seas around New Zealand — 1982. New Zealand J. Mar. Freshw. Res. 19 (1), 79–124, Publisher: Taylor & Francis.

Henley, S.F., Cavan, E.L., Fawcett, S.E., Kerr, R., Monteiro, T., Sherrell, R.M., Bowie, A.R., Boyd, P.W., Barnes, D.K., Schloss, I.R., Marshall, T., Flynn, R., Smith, S., 2020. Changing biogeochemistry of the southern ocean and its ecosystem implications. Front. Mar. Sci. 7 (July), 1–31, ISSN: 22967745.

Hernández-Ruiz, M., Barber-Lluch, E., Prieto, A., Álvarez-Salgado, X.A., Logares, R., Teira, E., 2018. Seasonal succession of small planktonic eukaryotes inhabiting surface waters of a coastal upwelling system. Environ. Microbiol. 20 (8), 2955–2973, Publisher: Wiley Online Library.

Holligan, P., Charalampopoulou, A., Hutson, R., 2010. Seasonal distributions of the coccolithophore, Emiliania huxleyi, and of particulate inorganic carbon in surface waters of the Scotia Sea. J. Mar. Syst. 82 (4), 195–205, Publisher: Elsevier.

Ibarbalz, F.M., Henry, N., Brandão, M.C., Martini, S., Busseni, G., Byrne, H., Coelho, L.P., Endo, H., Gasol, J.M., Gregory, A.C., Mahé, F., Rigonato, J., Royo-Llonch, M., Salazar, G., Sanz-Sáez, I., Scalco, E., Soviadan, D., Zayed, A.A., Zingone, A., Labadie, K., Ferland, J., Marec, C., Kandels, S., Picheral, M., Dimier, C., Poulain, J., Pisarev, S., Carmichael, M., Pesant, S., Babin, M., Boss, E., Iudicone, D., Jaillon, O., Acinas, S.G., Ogata, H., Pelletier, E., Stemmann, L., Sullivan, M.B., Sunagawa, S., Bopp, L., de Vargas, C., Karp-Boss, L., Wincker, P., Lombard, F., Bowler, C., Zinger, L., Acinas, S.G., Babin, M., Bork, P., Boss, E., Bowler, C., Cochrane, G., de Vargas, C., Follows, M., Gorsky, G., Grimsley, N., Guidi, L., Hingamp, P., Iudicone, D., Jaillon, O., Kandels, S., Karp-Boss, L., Karsenti, E., Not, F., Ogata, H., Pesant, S., Poulton, N., Raes, J., Sardet, C., Speich, S.,

Stemmann, L., Sullivan, M.B., Sunagawa, S., Wincker, P., 2019. Global trends in marine plankton diversity across kingdoms of life. Cell 179 (5), 1084–1097.e21.
Iida, T., Odate, T., 2014. Seasonal variability of phytoplankton biomass and composition in the major water masses of the Indian ocean sector of the Southern Ocean. Polar Sci. 8 (3), 283–297, Publisher: Elsevier.
Irion, S., Jardillier, L., Sassenhagen, I., Christaki, U., 2020. Marked spatiotemporal variations in small phytoplankton structure in contrasted waters of the Southern Ocean (Kerguelen area). Limnol. Oceanogr. 65 (11), 2835–2852, Publisher: Wiley Online Library.
Jang, S.H., Jeong, H.J., Lee, M.J., Kim, J.H., You, J.H., 2019. Gyrodinium jinhaense n. sp., a new heterotrophic unarmored dinoflagellate from the coastal waters of Korea. J. Euk. Microbiol. 66 (5), 821–835, Publisher: Wiley Online Library.
Jeong, H.J., Du Yoo, Y., Kim, J.S., Seong, K.A., Kang, N.S., Kim, T.H., 2010. Growth, feeding and ecological roles of the mixotrophic and heterotrophic dinoflagellates in marine planktonic food webs. Ocean Sci. J. 45 (2), 65–91, Publisher: Springer.
Jeong, H.J., Seong, K.A., Yoo, Y.D., Kim, T.H., Kang, N.S., Kim, S., Park, J.Y., Kim, J.S., Kim, G.H., Song, J.Y., 2008. Feeding and grazing impact by small marine heterotrophic dinoflagellates on heterotrophic bacteria. J. Euk. Microbiol. 55 (4), 271–288, Publisher: Wiley Online Library.
Jeong, H.J., Yoo, Y.D., Lee, K.H., Kim, T.H., Seong, K.A., Kang, N.S., Lee, S.Y., Kim, J.S., Kim, S., Yih, W.H., 2013. Red tides in masan bay, Korea in 2004–2005: I. Daily variations in the abundance of red-tide organisms and environmental factors. Harmful Algae 30, S75–S88.
Joglar, V., Álvarez-Salgado, X.A., Gago-Martinez, A., Leao, J.M., Pérez-Martínez, C., Pontiller, B., Lundin, D., Pinhassi, J., Fernández, E., Teira, E., 2021. Cobalamin and microbial plankton dynamics along a coastal to offshore transect in the Eastern North Atlantic Ocean. Environ. Microbiol. 23 (3), 1559–1583, Publisher: Wiley Online Library.
Johnson, M.D., Stoecker, D.K., Marshall, H.G., 2013. Seasonal dynamics of mesodinium rubrum in chesapeake bay. J. Plankton Res. 35 (4), 877–893, Publisher: Oxford University Press.
Koch, F., Marcoval, M.A., Panzeca, C., Bruland, K.W., Sanudo-Wilhelmy, S.A., Gobler, C.J., 2011. The effect of vitamin B12 on phytoplankton growth and community structure in the Gulf of Alaska. Limnol. Oceanogr. 56 (3), 1023–1034, Publisher: Wiley Online Library.
Lannuzel, D., Vancoppenolle, M., van der Merwe, P., de Jong, J., Meiners, K., Grotti, M., Nishioka, J., Schoemann, V., 2016. Iron in sea ice: Review and new insights. In: Deming, J.W., Miller, L.A. (Eds.), Elementa Sci. Anthropocene 4, 000130.
Latasa, M., Cabello, A.M., Morán, X.A.G., Massana, R., Scharek, R., 2017. Distribution of phytoplankton groups within the deep chlorophyll maximum. Limnol. Oceanogr. 62 (2), 665–685, ISBN: 1939-5590.
Latasa, M., Moran, A.G., Scharek, R., Estrada, M., 2005. Estimating the carbon flux through main phytoplankton groups in the northwestern Mediterranean. Limnol. Oceanogr. 50 (5), 1447–1458.
Latasa, M., Scharek, R., Morán, X.A.G., Gutiérrez-Rodríguez, A., Emelianov, M., Salat, J., Vidal, M., Estrada, M., 2022. Dynamics of phytoplankton groups in three contrasting situations of the open NW mediterranean Sea revealed by pigment, microscopy, and flow cytometry analyses. Prog. Oceanogr. 201, 102737, Publisher: Elsevier.
Latasa, M., Scharek, R., Vidal, M., Vila-Reixach, G., Gutiérrez-RodrÍguez, A., Emelianov, M., Gasol, J., 2010. Preferences of phytoplankton groups for waters of different trophic status in the northwestern Mediterranean sea. Mar. Ecol. Prog. Ser. 407.
Law, C.S., Breitbarth, E., Hoffmann, L.J., McGraw, C.M., Langlois, R.J., LaRoche, J., Marriner, A., Safi, K.a., 2012. No stimulation of nitrogen fixation by non-filamentous diazotrophs under elevated CO 2 in the South Pacific. Global Change Biol. 18 (10), 3004–3014, ISBN: 13541013.
Law, C., Smith, M., Stevens, C., Abraham, E., Ellwood, M., Hill, P., Nodder, S., Peloquin, J., Pickmere, S., Safi, K., Walkington, C., 2011. Did dilution limit the phytoplankton response to iron addition in HNLCLSi sub-antarctic waters during the SAGE experiment? Deep Sea Res. II Top. Stud. Oceanogr. 58 (6), 786–799.
Leblanc, K., Queguiner, B., Diaz, F., Cornet, V., Michel-Rodriguez, M., de Madron, X.D., Bowler, C., Malviya, S., Thyssen, M., Grégori, G., 2018. Nanoplanktonic diatoms are globally overlooked but play a role in spring blooms and carbon export. Nature Commun. 9 (1), 1–12, Publisher: Nature Publishing Group.
Legendre, L., Lefevre, J., 1995. Microbial food webs and the export of biogenic carbon in oceans. Aquat. Microb. Ecol. 9 (1), 69–77, ISBN: 0948-3055.
Leles, S., Mitra, A., Flynn, K., Stoecker, D., Hansen, P., Calbet, A., McManus, G., Sanders, R., Caron, D., Not, F., 2017. Oceanic protists with different forms of acquired phototrophy display contrasting biogeographies and abundance. Proc. R. Soc. B 284 (1860), 20170664, Publisher: The Royal Society.
Lemieux, C., Turmel, M., Otis, C., Pombert, J.-F., 2019. A streamlined and predominantly diploid genome in the tiny marine green alga Chloropicon primus. Nature Commun. 10 (1), 1–13, Publisher: Nature Publishing Group.
Liu, H., Probert, I., Uitz, J., Claustre, H., Aris-Brosou, S., Frada, M., Not, F., de Vargas, C., 2009. Extreme diversity in noncalcifying haptophytes explains a major pigment paradox in open oceans. Proc. Natl. Acad. Sci. USA 106 (31), 12803–12808.
Llopis Monferrer, N., Leynaert, A., Tréguer, P., Gutiérrez-Rodríguez, A., Moriceau, B., Gallinari, M., Latasa, M., L'Helguen, S., Maguer, J.-F., Safi, K., 2021. Role of small Rhizaria and diatoms in the pelagic silica production of the Southern Ocean. Limnol. Oceanogr. Publisher: Wiley Online Library.
Lomas, M.W., Roberts, N., Lipschultz, F., Krause, J.W., Nelson, D.M., Bates, N.R., 2009. Deep-sea research I biogeochemical responses to late-winter storms in the sargasso sea . IV . Rapid succession of major phytoplankton groups. Deep-Sea Res. 56, 892–908.
Longhurst, A.R., 2007. Ecological Geography of the Sea, 2nd ed. Ac p. 398.
Love, M.I., Huber, W., Anders, S., 2014. Moderated estimation of fold change and dispersion for RNA-seq data with DESeq2. Genome Biol. 15 (12), 1–21, Publisher: BioMed Central.
Mansour, J.S., Norlin, A., Llopis Monferrer, N., l'Helguen, S., Not, F., 2021. Carbon and nitrogen content to biovolume relationships for marine protist of the Rhizaria lineage (Radiolaria and Phaeodaria). Limnol. Oceanogr. 66 (5), 1703–1717, Publisher: Wiley Online Library.
Martiny, J.B.H., Bohannan, B.J.M., Brown, J.H., Colwell, R.K., Fuhrman, J.A., Green, J.L., Horner-Devine, M.C., Kane, M., Krumins, J.A., Kuske, C.R., Morin, P.J., Naeem, S., Øvreås, L., Reysenbach, A.-L., Smith, V.H., Staley, J.T., 2006. Microbial biogeography: putting microorganisms on the map. Nat. Rev. Microb. 4 (2), 102–112.
McMinn, A., Martin, A., Ryan, K., 2010. Phytoplankton and sea ice algal biomass and physiology during the transition between winter and spring (McMurdo Sound, Antarctica). Polar Biol. 33 (11), 1547–1556, Publisher: Springer.
McMurdie, P.J., Holmes, S., 2013. Phyloseq: An r package for reproducible interactive analysis and graphics of microbiome census data. PLoS One 8 (4), ISBN: 19326203 (ISSN).
Mestre, M., Ruiz-gonzález, C., Logares, R., Duarte, C.M., Gasol, J.M., 2018. Sinking particles promote vertical connectivity in the ocean microbiome. 115 (29), 6799–6807, ISBN: 1802470115.
Michaels, A.F., Caron, D.A., Swanberg, N.R., Howse, F.A., Michaels, C.M., 1995. Planktonic sarcodines (Acantaria, Radiolaria, Foraminifera) in surface waters near Bermuda: abundance, biomass and vertical flux. J. Plankton Res. 17, 131–163, ISBN: 0142-7873.
Mitra, A., Flynn, K.J., Burkholder, J.M., Berge, T., Calbet, A., Raven, J.A., Granéli, E., Glibert, P.M., Hansen, P.J., Stoecker, D.K., 2014. The role of mixotrophic protists in the biological carbon pump. Biogeosciences 11 (4), 995–1005, Publisher: Copernicus GmbH.
Mohan, R., Quarshi, A.A., Meloth, T., Sudhakar, M., 2011. Diatoms from the surface waters of the Southern Ocean during the austral summer of 2004. Current Sci. 1323–1327, Publisher: JSTOR.
Moline, M.A., Claustre, H., Frazer, T.K., Schofield, O., Vernet, M., 2004. Alteration of the food web along the Antarctic Peninsula in response to a regional warming trend. Global Change Biol. 10 (12), 1973–1980, Publisher: John Wiley & Sons, Ltd.
Morel, A., Maritorena, S., 2001. Bio-optical properties of oceanic waters: A reappraisal. J. Geophys. Res. Oceans 106, 7163–7180, Publisher: Wiley Online Library.
Murphy, R.J., Pinkerton, M.H., Richardson, K.M., Bradford-Grieve, J.M., Boyd, P.W., 2001. Phytoplankton distributions around New Zealand derived from SeaWiFS remotely-sensed ocean colour data. New Zealand J. Mar. Freshw. Res. 35 (2), 343–362, ISBN: 0028-8330.
Neil, H.L., Carter, L., Morris, M.Y., 2004. Thermal isolation of campbell plateau, New Zealand, by the antarctic circumpolar current over the past 130 kyr. Paleoceanography 19 (4), 1–17, ISBN: 0883-8305.
Nodder, S.D., Chiswell, S.M., Northcote, L.C., 2016. Annual cycles of deep-ocean biogeochemical export fluxes in subtropical and subantarctic waters, southwest Pacific ocean. J. Geophys. Res. Oceans 121 (4), 2405–2424, Publisher: Wiley Online Library.
Nunes, S., Latasa, M., Delgado, M., Emelianov, M., Simó, R., Estrada, M., 2019. Phytoplankton community structure in contrasting ecosystems of the southern ocean: South georgia, south orkneys and western antarctic peninsula. Deep Sea Res. I Oceanogr. Res. Pap. 151, 103059.
Nunes, S., Latasa, M., Gasol, J., Estrada, M., 2018. Seasonal and interannual variability of phytoplankton community structure in a Mediterranean coastal site. Mar. Ecol. Prog. Ser. 592, 57–75.
Ohman, M.D., Powell, J.R., Picheral, M., Jensen, D.W., 2012. Mesozooplankton and particulate matter responses to a deep-water frontal system in the southern California Current System. J. Plankton Res. 34 (9), 815–827.
Oksanen, J., Blanchet, G., Friendly, M., Kindt, R., Legendre, P., McGlinn, D., Minchin, P.R., O'Hara, R., Simpson, G., Solymos, P., Stevens, H., Szoecs, E., Wagner, H., 2019. Vegan: Community ecology package. R package version 2.5–6. 2019.
Olguín, H.F., Alder, V.A., 2011. Species composition and biogeography of diatoms in antarctic and subantarctic (Argentine shelf) waters (37–76 s). Deep Sea Res. II Top. Stud. Oceanogr. 58 (1), 139–152, Publisher: Elsevier.
Ollison, G.A., Hu, S.K., Mesrop, L.Y., DeLong, E.F., Caron, D.A., 2021. Come rain or shine: Depth not season shapes the active protistan community at station ALOHA in the north Pacific subtropical gyre. Deep Sea Res. I Oceanogr. Res. Pap. 170, 103494, URL https://www.sciencedirect.com/science/article/pii/S0967063721000339.
Olson, M.B., Strom, S.L., 2002. Phytoplankton growth, microzooplankton herbivory and community structure in the southeast bering sea: insight into the formation and temporal persistence of an emiliania huxleyi bloom. Deep-Sea Res. II-Top. Stud. Oceanogr. 49 (26), 5969–5990, ISBN: 0967-0645.

Paerl, R., Bertrand, E., Allen, A., Palenik, B., Azam, F., 2015. Vitamin B1 ecophysiology of marine picoeukaryotic algae: strain-specific differences and a new role for bacteria in vitamin cycling. Limnol. Oceanogr. 60 (1), 215–228, Publisher: Wiley Online Library.

Panzeca, C., Tovar-Sanchez, A., Agustí, S., Reche, I., Duarte, C.M., Taylor, G.T., Sañudo Wilhelmy, S.A., 2006. B vitamins as regulators of phytoplankton dynamics. EOS Trans. Am. Geophys. Union 87 (52), 593–596, Publisher: Wiley Online Library.

Peloquin, J., Hall, J., Safi, K., Smith, W.O., Wright, S., van den Enden, R., 2011. The response of phytoplankton to iron enrichment in sub-antarctic HNLCLSi waters: Results from the SAGE experiment. Deep Sea Res. II Top. Stud. Oceanogr. 58 (6), 808–823, ISBN: 09670645.

Pernice, M.C., Forn, I., Gomes, A., Lara, E., Alonso-Sáez, L., Arrieta, J.M., del Carmen Garcia, F., Hernando-Morales, V., MacKenzie, R., Mestre, M., 2015. Global abundance of planktonic heterotrophic protists in the deep ocean. ISME J. 9 (3), 782–792, Publisher: Nature Publishing Group.

Pernice, M.C., Giner, C.R., Logares, R., Perera-Bel, J., Acinas, S.G., Duarte, C.M., Gasol, J.M., Massana, R., 2016. Large variability of bathypelagic microbial eukaryotic communities across the world's oceans. ISME J. 10 (4), 945–958, Publisher: Nature Publishing Group.

Pinkernell, S., Beszteri, B., 2014. Potential effects of climate change on the distribution range of the main silicate sinker of the southern ocean. Ecol. Evol. 4 (16), 3147–3161, Publisher: John Wiley & Sons, Ltd.

Pinkerton, M.H., Richardson, K.M., Boyd, P.W., Gall, M.P., Zeldis, J., Oliver, M.D., Murphy, R.J., 2005. Intercomparison of ocean colour band-ratio algorithms for chlorophyll concentration in the Subtropical front east of New Zealand. Remote Sens. Environ. 97 (3), 382–402.

Piredda, R., Tomasino, M.P., D'Erchia, A.M., Manzari, C., Pesole, G., Montresor, M., Kooistra, W.H., Sarno, D., Zingone, A., 2017. Diversity and temporal patterns of planktonic protist assemblages at a Mediterranean Long Term Ecological Research site. FEMS Microb. Ecol. 93 (1), ISBN: 1574-6941 (Electronic) 0168-6496 (Linking).

Piwosz, K., Wiktor, J.M., Niemi, A., Tatarek, A., Michel, C., 2013. Mesoscale distribution and functional diversity of picoeukaryotes in the first-year sea ice of the Canadian Arctic. ISME J. 7 (8), 1461–1471, Publisher: Nature Publishing Group.

Pörtner, H.-O., Karl, D.M., Boyd, P.W., Cheung, W., Lluch-Cota, S.E., Nojiri, Y., Schmidt, D.N., Zavialov, P.O., Alheit, J., Aristegui, J., 2014. Ocean systems. In: Climate Change 2014: Impacts, Adaptation, and Vulnerability. Part a: Global and Sectoral Aspects. Contribution of Working Group II To the Fifth Assessment Report of the Intergovernmental Panel on Climate Change. Cambridge University Press, pp. 411–484.

Prebble, J., Crouch, E., Carter, L., Cortese, G., Nodder, S., 2013. Dinoflagellate cysts from two sediment traps east of New Zealand. Mar. Micropaleontol. 104, 25–37, Publisher: Elsevier.

Preston, C.M., Durkin, C.A., Yamahara, K.M., 2020. DNA metabarcoding reveals organisms contributing to particulate matter flux to abyssal depths in the North East Pacific ocean. Deep Sea Res. II Top. Stud. Oceanogr. 173.

Quéguiner, B., Tréguer, P., Peeken, I., Scharek, R., 1997. Biogeochemical dynamics and the silicon cycle in the atlantic sector of the Southern Ocean during austral spring 1992. Deep Sea Res. II Top. Stud. Oceanogr. 44 (1), 69–89, Publisher: Elsevier.

Raes, E.J., Bodrossy, L., Van De Kamp, J., Bissett, A., Ostrowski, M., Brown, M.V., Sow, S.L., Sloyan, B., Waite, A.M., 2018. Oceanographic boundaries constrain microbial diversity gradients in the South Pacific Ocean. Proc. Natl. Acad. Sci. 115 (35), E8266–E8275, Publisher: National Acad Sciences.

Rigual-Hernández, A., Trull, T., Bray, S., Cortina, A., Armand, L., 2015. Latitudinal and temporal distributions of diatom populations in the pelagic waters of the Subantarctic and Polar Frontal zones of the Southern Ocean and their role in the biological pump. Biogeosciences 12 (18), 5309–5337, Publisher: Copernicus GmbH.

Rigual-Hernández, A.S., Trull, T.W., Flores, J.A., Nodder, S.D., Eriksen, R., Davies, D.M., Hallegraeff, G.M., Sierro, F.J., Patil, S.M., Cortina, A., Ballegeer, A.M., Northcote, L.C., Abrantes, F., Rufino, M.M., 2020. Full annual monitoring of Subantarctic Emiliania huxleyi populations reveals highly calcified morphotypes in high-CO2 winter conditions. Sci. Rep. 10 (1), 2594.

Rodríguez, F., Derelle, E., Guillou, L., Le Gall, F., Vaulot, D., Moreau, H., 2005. Ecotype diversity in the marine picoeukaryote Ostreococcus (Chlorophyta, Prasinophyceae). Environ. Microbiol. 7 (6), 853–859, Publisher: Wiley Online Library.

Roemmich, D., Sutton, P., 1998. The mean and variability of ocean circulation past northern new Zealand: Determining the representativeness of hydrographic climatologies. J. Geophys. Res. Oceans 103, 13041–13054, Publisher: Wiley Online Library.

Ruiz-Gonzalez, C., Mestre, M., Estrada, M., Sebastian, M., Salazar, G., Agust, S., Moreno-Ostos, E., Reche, I., Alvarez-Salgado, X.A., Moran, X.A.G., Duarte, C.M., Sala, M.M., Gasol, J.M., 2020. Major imprint of surface plankton on deep ocean prokaryotic structure and activity. Mol. Ecol. 29 (10), 1820–1838.

Saavedra-Pellitero, M., Baumann, K.-H., Flores, J.-A., Gersonde, R., 2014. Biogeographic distribution of living coccolithophores in the Pacific sector of the southern ocean. Mar. Micropaleontol. 109, 1–20.

Saito, H., Ota, T., Suzuki, K., Nishioka, J., Tsuda, A., 2006. Role of heterotrophic dinoflagellate Gyrodinium sp in the fate of an iron induced diatom bloom. Geophys. Res. Lett. 33 (9).

Santana, R., Suanda, S.H., Macdonald, H., O'Callaghan, J., 2021. Mesoscale and wind-driven intra-annual variability in the East Auckland Current. Sci. Rep. 11 (1), 1–11, Publisher: Nature Publishing Group.

Santoferrara, L., Burki, F., Filker, S., Logares, R., Dunthorn, M., McManus, G.B., 2020. Perspectives from ten years of protist studies by high-throughput metabarcoding. J. Euk. Microbiol. jeu.12813, Publisher: Wiley.

Lopes dos Santos, A., Gourvil, P., Tragin, M., Noël, M.-H., Decelle, J., Romac, S., Vaulot, D., 2017a. Diversity and oceanic distribution of prasinophytes clade VII, the dominant group of green algae in oceanic waters. ISME J. 11 (2), 512–528.

Lopes dos Santos, A., Pollina, T., Gourvil, P., Corre, E., Marie, D., Garrido, J.L., Rodríguez, F., No el, M.-H., Vaulot, D., Eikrem, W., 2017b. Chloropicophyceae, a new class of picophytoplanktonic prasinophytes. Sci. Rep. 7 (1), 1–20, Publisher: Nature Publishing Group.

Sarmiento, J.L., Slater, R., Barber, R., Bopp, L., Doney, S.C., Hirst, a.C., Kleypas, J., Matear, R., Mikolajewicz, U., Monfray, P., Soldatov, V., Spall, S.a., Stouffer, R., 2004. Response of ocean ecosystems to climate warming. Glob. Biogeochem. Cycles 18 (3), n/a–n/a.

Sato, M., Takeda, S., Furuya, K., 2009. Responses of pico- and nanophytoplankton to artificial iron infusions observed during the second iron enrichment experiment in the western subarctic Pacific (SEEDS II). Deep-Sea Res. II Top. Stud. Oceanogr. 56 (26), 2745–2754.

Schneider, L.K., Anestis, K., Mansour, J., Anschütz, A.A., Gypens, N., Hansen, P.J., John, U., Klemm, K., Martin, J.L., Medic, N., 2020. A dataset on trophic modes of aquatic protists. Biodiver. Data J. 8, Publisher: Pensoft Publishers.

Schofield, O., Saba, G., Coleman, K., Carvalho, F., Couto, N., Ducklow, H., Finkel, Z., Irwin, A., Kahl, A., Miles, T., Montes-Hugo, M., Stammerjohn, S., Waite, N., 2017. Decadal variability in coastal phytoplankton community composition in a changing west antarctic peninsula. Deep Sea Res. I Oceanogr. Res. Pap. 124, 42–54.

Seymour, J.R., Doblin, M.A., Jeffries, T.C., Brown, M.V., Newton, K., Ralph, P.J., Baird, M., Mitchell, J.G., 2012. Contrasting microbial assemblages in adjacent water masses associated with the east Australian current. Environ. Microbiol. Rep. 4 (5), 548–555, Publisher: John Wiley & Sons, Ltd.

Sherlock, V., Pickmere, S., Currie, K., Hadfield, M., Nodder, S., Boyd, P., 2007. Predictive accuracy of temperature-nitrate relationships for the oceanic mixed layer of the New Zealand region. J. Geophys. Res. Oceans 112, Publisher: Wiley Online Library.

Sherr, E.B., Sherr, B.F., 2007. Heterotrophic dinoflagellates: a significant component of microzooplankton biomass and major grazers of diatoms in the sea. Mar. Ecol. Prog. Ser. 352, 187–197.

Shi, X.L., Marie, D., Jardillier, L., Scanlan, D.J., Vaulot, D., 2009. Groups without cultured representatives dominate eukaryotic picophytoplankton in the oligotrophic South East Pacific Ocean. PLoS One 4 (10), e7657, Publisher: Public Library of Science San Francisco, USA.

Smith, R.O., Vennell, R., Bostock, H.C., Williams, M.J., 2013. Interaction of the subtropical front with topography around southern New Zealand. Deep Sea Res. I Oceanogr. Res. Pap. 76, 13–26, Publisher: Elsevier.

Sow, L.S.S., Trull, T.W., Bodrossy, L., 2020. Oceanographic fronts shape phaeocystis assemblages: A high-resolution 18S rRNA gene survey from the ice-edge to the equator of the south pacific. Front. Microbiol. 11, 1847.

Moon-van der Staay, S.Y., De Wachter, R., Vaulot, D., 2001. Oceanic 18S rDNA sequences from picoplankton reveal unsuspected eukaryotic diversity. Nature 409 (6820), 607–610, Publisher: Nature Publishing Group.

Stanton, B.R., Morris, M.Y., 2004. Direct velocity measurements in the Subantarctic Front and over Campbell Plateau, southeast of New Zealand. J. Geophys. Res. Oceans 109, Publisher: Wiley Online Library.

Stanton, B.R., Sutton, P.J., Chiswell, S.M., 1997. The east auckland current, 1994–95. New Zealand J. Mar. Freshw. Res. 31 (4), 537–549, Publisher: Taylor & Francis.

Strom, S.L., Brainard, M.A., Holmes, J.L., Olson, M.B., 2001. Phytoplankton blooms are strongly impacted by microzooplankton grazing in coastal North Pacific waters. Mar. Biol. 138 (2), 355–368, ISBN: 0025-3162.

Stukel, M.R., Ohman, M.D., Kelly, T.B., Biard, T., 2019. The roles of suspension-feeding and flux-feeding zooplankton as gatekeepers of particle flux into the mesopelagic ocean in the northeast pacific. Front. Mar. Sci. 6.

Sutton, P., 2001. Detailed structure of the subtropical front over Chatham Rise, east of New Zealand. J. Geophys. Res. Oceans 106, 31045–31056, Publisher: Wiley Online Library.

Sutton, P.J., 2003. The southland current: a subantarctic current. New Zealand J. Mar. Freshw. Res. 37 (3), 645–652, Publisher: Taylor & Francis.

Sutton, P.J., Bowen, M., 2014. Flows in the Tasman front south of Norfolk island. J. Geophys. Res. Oceans 119 (5), 3041–3053, Publisher: Wiley Online Library.

Suzuki, N., Not, F., 2015. In: Ohtsuka, S., Suzaki, T., Horiguchi, T., Suzuki, N., Not, F. (Eds.), Biology and Ecology of Radiolaria. Springer, pp. 179–222.

Suzuki, K., Saito, H., Isada, T., Hattori-Saito, A., Kiyosawa, H., Nishioka, J., McKay, R.M.L., Kuwata, A., Tsuda, A., 2009. Community structure and photosynthetic physiology of phytoplankton in the northwest subarctic Pacific during an in situ iron fertilization experiment (SEEDS-II). Deep Sea Res. II Top. Stud. Oceanogr. 56 (26), 2733–2744, Publisher: Elsevier.

Swan, C.M., Vogt, M., Gruber, N., Laufkoetter, C., 2016. A global seasonal surface ocean climatology of phytoplankton types based on CHEMTAX analysis of HPLC pigments. Deep Sea Res. I Oceanogr. Res. Pap. 109, 137–156, ISBN: 09670637.

Takahashi, K., 1983. Radiolaria - sinking population, standing stock, and production-rate. Mar. Micropaleontol. 8 (3), 171–181, ISBN: 0377-8398.

Techtmann, S.M., Fortney, J.L., Ayers, K.A., Joyner, D.C., Linley, T.D., Pfiffner, S.M., Hazen, T.C., 2015. The unique chemistry of eastern mediterranean water masses selects for distinct microbial communities by depth. PLoS One 10 (3), e0120605, Publisher: Public Library of Science.

Thiele, S., Wolf, C., Schulz, I.K., Assmy, P., Metfies, K., Fuchs, B.M., 2014. Stable composition of the nano-and picoplankton community during the ocean iron fertilization experiment LOHAFEX. PLoS One 9 (11), e113244, Publisher: Public Library of Science San Francisco, USA.

Timmermans, K., Van der Wagt, B., Veldhuis, M., Maatman, A., De Baar, H., 2005. Physiological responses of three species of marine pico-phytoplankton to ammonium, phosphate, iron and light limitation. J. Sea Res. 53 (1), 109–120, Publisher: Elsevier.

Tragin, M., Vaulot, D., 2018. Green microalgae in marine coastal waters: The ocean sampling day (OSD) dataset. Sci. Rep. 8 (1), 14020.

Tragin, M., Vaulot, D., 2019. Novel diversity within marine Mamiellophyceae (Chlorophyta) unveiled by metabarcoding. Sci. Rep. 9 (1), 5190.

Trefault, N., De la Iglesia, R., Moreno-Pino, M., Lopes dos Santos, A., Gérikas Ribeiro, C., Parada-Pozo, G., Cristi, A., Marie, D., Vaulot, D., 2021. Annual phytoplankton dynamics in coastal waters from fildes bay, western antarctic peninsula. Sci. Rep. 11 (1), 1368.

Trull, T.W., Sedwick, P.N., Griffiths, F.B., Rintoul, S.R., 2001. Introduction to special section: SAZ project. J. Geophys. Res.-Oceans 106, 31425–31429.

Turner, J.T., 2015. Zooplankton fecal pellets, marine snow, phytodetritus and the ocean's biological pump. Prog. Oceanogr. 130, 205–248, ISBN: 00796611.

Twining, B.S., Nodder, S.D., King, A.L., Hutchins, D.A., LeCleir, G.R., DeBruyn, J.M., Maas, E.W., Vogt, S., Wilhelm, S.W., Boyd, P.W., 2014. Differential remineralization of major and trace elements in sinking diatoms. Limnol. Oceanogr. 59 (3), 689–704, ISBN: 0024-3590.

Uitz, J., Claustre, H., Morel, A., Hooker, S.B., 2006. Vertical distribution of phytoplankton communities in open ocean: An assessment based on surface chlorophyll. J. Geophys. Res. Oceans 111, Publisher: John Wiley & Sons, Ltd.

Vargas, C.D., Audic, S., Henry, N., Decelle, J., Mahé, F., Logares, R., Lara, E., Berney, C., Bescot, N.L., Probert, I., Carmichael, M., Poulain, J., Romac, S., 2015. Eukaryotic plankton diversity in the sunlit ocean. Science 348 (6237), 1–12.

Verity, P.G., Brussaard, C.P., Nejstgaard, J.C., van Leeuwe, M.A., Lancelot, C., Medlin, L.K., 2007. Current understanding of phaeocystis ecology and biogeochemistry, and perspectives for future research. Biogeochemistry 83 (1), 311–330, Publisher: Springer.

Vidussi, F., Claustre, H., Manca, B.B., Luchetta, A., Marty, J.-C., 2001. Phytoplankton pigment distribution in relation to upper thermocline circulation in the eastern mediterranean sea during winter. J. Geophys. Res. Oceans 106, 19939–19956, Publisher: John Wiley & Sons, Ltd.

Vidussi, F., Marty, J.-c., Chiave, J., 2000. Phytoplankton pigment variations during the transition from spring bloom to oligotrophy in the northwestern Mediterranean sea. Deep-Sea Res. 47, ISBN: 0014187241842.

Wang, Q., Garrity, G.M., Tiedje, J.M., Cole, J.R., 2007. Naive Bayesian classifier for rapid assignment of rRNA sequences into the new bacterial taxonomy. Appl. Environ. Microbiol. 73 (16), 5261–5267, Edition: 2007/06/22 Publisher: American Society for Microbiology.

Wietz, M., Lau, S.C., Harder, T., 2019. Editorial: Socio-ecology of microbes in a changing ocean. Front. Mar. Sci. 6, 190, URL https://www.frontiersin.org/article/10.3389/fmars.2019.00190.

Sañudo Wilhelmy, S.A., Gómez-Consarnau, L., Suffridge, C., Webb, E.A., 2014. The role of b. vitamins in marine biogeochemistry. Ann. Rev. Mar. Sci. 6, 339–367, Publisher: Annual Reviews.

Wilks, J.V., Nodder, S.D., Rigual-Hernandez, A., 2021. Diatom and coccolithophore species fluxes in the subtropical frontal zone, east of New Zealand. Deep Sea Res. I Oceanogr. Res. Pap. 169, 103455, Publisher: Elsevier.

Wolf, C., Frickenhaus, S., Kilias, E.S., Peeken, I., Metfies, K., 2014. Protist community composition in the Pacific sector of the southern ocean during austral summer 2010. Polar Biol. 37 (3), 375–389, ISBN: 0722-4060; 1432-2056 tex.mendeley-tags: Micromonas.

Zeldis, J.R., Décima, M., 2020. Mesozooplankton connect the microbial food web to higher trophic levels and vertical export in the New Zealand subtropical convergence zone. Deep Sea Res. I Oceanogr. Res. Pap. 155, 103146.

Zentara, S., Kamykowski, D., 1981. Geographic variations in the relationship between silicic acid and nitrate in the South Pacific Ocean. Deep Sea Res. A 28, 455–465, tex.address: AA(1110 Brookgreen Drive, Cary, NC 27511, U.S.A.), AB(Department of Marine Science and Engineering, North Carolina State University, Raleigh, NC 27650, U.S.A.).

Zhu, F., Massana, R., Not, F., Marie, D., Vaulot, D., 2005. Mapping of picoeucaryotes in marine ecosystems with quantitative PCR of the 18S rRNA gene. FEMS Microbiol. Ecol. 52 (1), 79–92, Publisher: Blackwell Publishing Ltd Oxford, UK.

Zoccarato, L., Pallavicini, A., Cerino, F., Fonda Umani, S., Celussi, M., 2016. Water mass dynamics shape ross sea protist communities in mesopelagic and bathypelagic layers. Prog. Oceanogr. 149, 16–26, Publisher: Elsevier Ltd.